IIT BOMBAY NCAIR NATIONAL CENTRE FOR AEROSPACE INNOVATION AND RESEARCH

#TR/2015/0X

TRACTION MODEL DEVELOPMENT FOR MULTI-AXIS BALL END MILLING PROCESSES

Deepak Kumar Pawar

Taha S. Khot

JUNE 2014 - SEPTEMBER 2015

Reviewed by : **TAHA S. KHOT (NCAIR)**

Approved by : **ASIM TEWARI (IIT Bombay)**

Published at :

Distributed to :

EXECUTIVE SUMMARY

Precision machining is widely used in several manufacturing industries today. In certain sectors such as aerospace and defense, accuracy and quality of machined parts is of prime importance in order to ensure optimal performance. However there are challenges which affect productivity such as parts having complex free-form surfaces, and characteristics of difficult-to-machine materials such as Titanium and Inconel. Hence it is necessary to look for ways to optimize the machining process.

One method is to model and analyze the forces and torque that are generated during machining since they significantly affect the performance of the cutting process as well as the surface quality of the machined part. Furthermore, these forces are highly dynamic and lead to vibrations and chatter while the part is being machined.

In this project two approaches have been employed to model the cutting forces generated during multi-axis ball-end milling processes. These are based on an empirical mechanistic methodology and a physics-based analytical methodology. With the help of these models, for a given set of machining parameters the cutting forces and torque can be predicted very quickly and with fairly good accuracy.

A GUI based application program is developed which allows the user to simulate and observe the performance of milling processes. This can further be used to optimize several aspects of the machining process from tool-geometry design or selection and process parameter optimization. Optimizing the cutting process will not only improve the speed of machining, but also help in achieving better accuracy of the machined parts.

TABLE OF CONTENTS

List of Figures

List of Tables

Nomenclature

FCN	Feed coordinate system
TCS	Tool coordinate system
LCS	Local coordinate system
N_f	Number of cutting edge(s)
R_0	Ball end mill radius
Z	axial distance from tool tip
$r(z)$	Local radius of the ball end mill in xy plane
K	Axial immersion angle
Ψ	Lag angle
Φ	Radial immersion angle
i_o	Helix angle at ball shank interface
θ	Tool rotation angle (measured from +y axis CW)
Φ_p	Pitch angle
$xx_{tcs}(z)$	X coordinates in TCS coordinates system
$yy_{tcs}(z)$	Y coordinates in TCS coordinates system
$zz_{tcs}(z)$	Z coordinates in TCS coordinates system
$d\theta$	Angular increment
dz	Axial increment
K_p	Angular integration points
L_p	Axial integration points
T	Transformation matrix from TCS to FCN coordinates
$lead$	Lead angle
$tilt$	Tilt angle
S_t	Feed per cutting edge
$t_n(\Psi, \theta, \mathrm{K})$	Chip thickness
db	Chip width
ds	Chip length
r	Chip compression ratio/cutting ratio
τ	Shear stress
φ	Shear angle

φ_n	Normal shear angle in oblique cutting
β	Average friction angle at the rake face in orthogonal
β_n	Normal friction angle
α_0	Orthogonal rake angle
α_n	Normal rake angle
r	Orthogonal chip thickness ratio
r_t	Equivalent chip thickness ratio in oblique cutting
η_c	Chip flow angle
$K_{tc}\ K_{rc}\ K_{ac}$	Tangential, radial and axial cutting force coefficients
$K_{te}\ K_{re}\ K_{ae}$	Tangential, radial and axial edge force coefficients
$dF_t\ dF_r\ \ dF_a$	Differential cutting forces in LCS
$dF_x\ dF_y\ \ dF_z$	Differential cutting forces in LCS
$F_x\ F_y\ F_z$	Milling forces in Cartesian coordinate system
n	Spindle speed in rpm
doc	Depth of cut

1. INTRODUCTION

Precision machining is perhaps one of the most essential and widely performed manufacturing process in several industries today, particularly in the aerospace and automotive sectors. It is amongst the few conventional manufacturing processes which ensures that raw materials are converted efficiently into functional parts within the tolerance limits set by design.

As a result of continuous technological advancements in the last few decades, the demand for complex multi-axis parts manufactured to high precision and quality has risen significantly. Further, the advent of new and superior materials is posing newer challenges to manufacturing processes. High technology sectors such as aerospace and defense are widely using Titanium and Inconel to make complex parts such as turbine blades, blisks, dies and moulds. These materials, which possess excellent mechanical properties, are however difficult to process. This makes manufacturing a great challenge which as a result affects production and output.

Machining, particularly milling, is a highly dynamic process. The cutting loads (forces and torque) generated during the process involve high-frequency periodic fluctuations as the tool spins and engages with the workpiece. These forces depend on several factors such as—

- Design of the cutting tool geometry
- Machining process parameters— speed, feed, cutting depth, and tool-orientation
- Work piece material and environmental characteristics.

The magnitude and periodicity of the forces has a direct impact on the performance of the cutting process, especially with regards to tool wear-out (which affects tool life), machined surface roughness, and part-tool vibrations. The tool-life essentially governs the duration for which a given tool can be used without deterioration in quality and accuracy of the machined part. The surface roughness is a measure of the surface quality of the finished part which determines the deviation of the machined surface from the nominal (desired) surface profile. This again depends on the cutting forces generated and the tool wear-out. The vibrations in the tool and workpiece are a result

of the magnitudes and periodicity of the cutting forces as well as the design and stiffness. This leads to deteriorated surface roughness as a result of non-uniform or irregular cutting caused due to the vibrations.

Hence it is essential to possess a clear understanding of how these forces are generated during the cutting process. A scheme for modeling the cutting process must therefore be developed in order to predict the cutting loads with sufficient accuracy. This could then be used to optimize several aspects of the machining process from tool-geometry design or selection, to toolpath planning, and process parameter optimization. Optimizing the cutting process will not only improve the speed of machining, but will also help in achieving better accuracy and reduced tool wear-out.

1.1 Objective of the project

The main aim of the project is to develop a methodology to predict cutting forces and torque generated during multi-axis ball-end milling processes. This is to be accomplished by modeling the cutting tool geometry and its orientation with respect to the workpiece, and integrating with the material models which define the cutting process. Based on the geometry and material models, the forces and torque are to be computed using a mechanistic approach and a physics based mathematical approach. The mechanistic methodology involves an empirical approach in which the basic orthogonal cutting parameters are estimated using a regression curve-fitting on several measured cutting test results. On the other hand, the physics based methodology employs an analytical modeling approach in which the behavior of the material undergoing cutting is predicted using the Johnson-Cook material model. Both approaches are described in subsequent sections.

Running the models would compute the variation in the forces and torque as a function of the tool rotation. Further, the predicted forces are to be benchmarked against data in published literature and also using experimental data. The modelled forces can then be used to predict tool wear-out and vibrations in the tool and workpiece, which will be taken up in the subsequent phases of the project.

1.2 Overall Approach

A modular approach is developed and employed to model the milling process. The milling process is split into different modules, with each module modelled individually before being integrated together to obtain the forces and torque. This is explained with the help of the following chart:

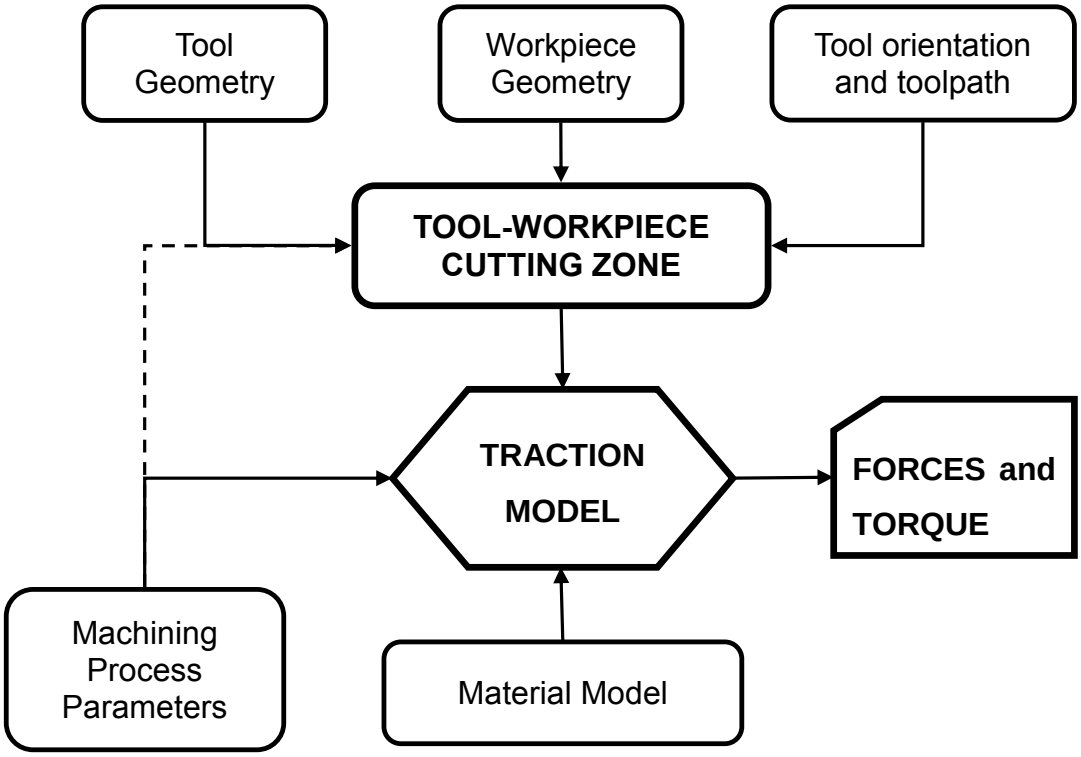

Figure 1 Overall modeling approach

parametrically using various mathematical formulations. The complex tool geometry is discretized into several infinitesimal elements on which the subsequent force analysis will be performed. Then based on the direction of the toolpath (feed direction) and the discretized tool geometry, the portion of the cutting tool which is in contact with the workpiece (*cutting-zone)* is identified (i.e. portion of the tool actually removing the uncut material).

A constitutive *material model* is developed both mechanistically as well as analytically to predict its mechanical characteristics during the cutting process. The material model, along with the user-specified machining process parameters, and the identified

zone are used as inputs to what is called as the *Traction Model.* The traction model is essentially an integration of the geometric, process, and the material models. The output from the Traction Model are the forces and torque acting on the cutting tool.

1.3 Project Outcomes

The primary outcome of the project is an application program which allows the user to simulate the performance of milling processes. The user inputs the tool geometry and machining process parameters, and the program computes the different cutting forces and torque as a function of tool rotation. The program can be used to understand how the forces and torque vary as the tool engages the workpiece. It can also be used to study the effect of the tool geometry, tool-orientation and process parameters on the magnitude of the forces and torque.

A GUI has been developed through with which the user can easily define and edit inputs to the program. It also includes a lead-tilt range explorer which can be used to identify optimal combinations of tool orientation angles (lead and tilt) where the cutting forces are minimum.

###

2. METHODOLOGY A— EMPIRICAL MODEL BASED APPROACH

The first methodology employs a mechanistic approach to model the cutting forces. Its basis lies in establishing an empirical relationship in which the basic orthogonal cutting parameters are estimated using regression curve-fitting of several measured cutting test data. This empirical relationship is then used to compute cutting force coefficients which are subsequently used to calculate the forces and torque.

In general, cutting forces are generated due to two processes—a primary process which includes shearing of the work material in the shear zone, and a secondary process which involves rubbing or ploughing at the cutting edge. There are coefficients which are associated with each process— Cutting force coefficients based on primary process, and Edge coefficients due to secondary forces. In this methodology both of these coefficients are computed using the empirical relationships obtained from the test data.

The next involves modeling of the cutting tool geometry and its orientation with respect to the workpiece and the feed direction. The cutting edges of the tool are discretized into several infinitesimal elements with each of them undergoing oblique cutting. Using these elements along with the machining process parameters, the dimensions of the un-deformed chip are obtained. These dimensions are subsequently used with the force and edge coefficients to obtain the differential cutting forces which are then integrated to give the net forces and torque acting on the tool. In order to validate the model, the predicted forces are compared with data obtain from published literature as well experimental tests.

Furthermore, based on this methodology, a Milling Process Simulator (MPS) program is written. Using MPS, for a given ball-end mill geometry and set of machining process parameters, the user can evaluate the performance of the milling process.

Subsequent sections in this chapter explain the entire process of computing the cutting forces, beginning with the geometrical modeling of the tool, identification of the cutting zone, computing the coefficients, and finally calculating the forces and torques. The chapter concludes with model validation studies and a brief description of MPS.

2.1 Geometric Modelling of Ball-end Mill

In order to model and predict cutting forces, the first step is the geometric modeling of the milling tool. There are several geometric features such as tool diameter; helix and rake angles, which govern the performance of the milling process. Hence, these features must be modelled accurately before integrating them with the force model.

The approach involves establishing all coordinate systems required to model the entire process. This includes one coordinate system for the workpiece and the toolpath which essentially defines the feed and work surface normal directions, and two coordinate systems for modelling the cutting tool. All three coordinate systems can be related to one another, and the modelled data can be transferred from one coordinate system to the other via transformation matrices.

Once all coordinate systems are defined, the tool is modelled by expressing its helical cutting edges using a mathematical formulation. The tool surface envelope, which is the area swept by the cutting edge as it rotates about the tool axis, is then discretized to obtain infinitesimal cutting elements. The elements which lie within the cutting zone (described in subsequent sections) are then to be used as inclined cutting edges undergoing oblique cutting, and subsequently the forces and torque can be computed.

2.1.1 Coordinate Systems

Modelling of 5-axis machining process requires the definition of three coordinate systems. These are required in order to define the angular orientation of the tool axis with respect to the workpiece.

First is the Feed Coordinate System (FCN) for which the axes are defined using the feed direction (F), work piece surface normal (N) and the cross feed direction(C). Second is the Tool Coordinate System (TCS) where the cutting tool axis is along the (z) axis, (x) and (y) axes are in the transversal directions of the cutting tool.

Third is the Local Coordinate System (LCS) which defines the, radial, tangential, and axial directions of individual cutting elements of the tool.

2.1.2 Cutting Edge Geometric Parameters

For a ball end mill, the cutting edges lie on a hypothetical hemispherical surface of radius R_0. They also extend along the shank surface depending on the geometry definition of the tool. Furthermore, the cutting edges also twist from the tool tip upwards along the tool axis. This twist is defined using the helix angle i_0 of the tool (usually defined at the ball-shank interface). The expression for the envelope of ball end part is given as:

$$x^2 + y^2 + (R_0 - z)^2 = R_0^2 \quad (1)$$

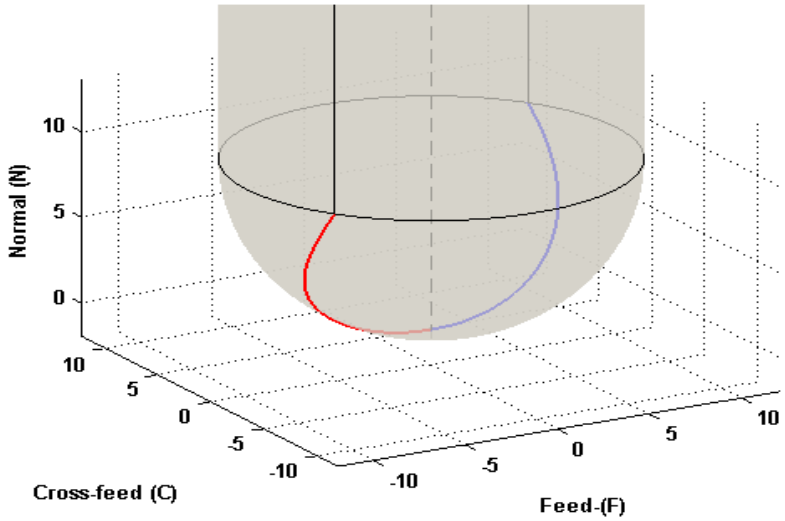

Figure 2 Helical cutting edges on ball end mill envelope

To model the cutting edge the following geometric parameters must be defined:

- Axial distance from tool tip (Z)
- Local radius $r(\Psi(z))$
- Axial immersion angle (K)
- Lag angle (Ψ)
- Radial immersion angle (Φ)

The local radius of the ball end mill changes with the axial distance from the ball tip. This variation in a local radius is expressed as follows :

$$r(z) = \sqrt{R_0^2 - (R_0 - z)^2} \tag{2}$$

The axial immersion angle (*K*), is defined as the angle between the tool axis and normal of the infinitesimal cutting edge/cutting point. The axial immersion angle can be expressed as follows: (Figure 2)

$$K = \sin^{-1}\frac{r(z)}{R_0} \tag{3}$$

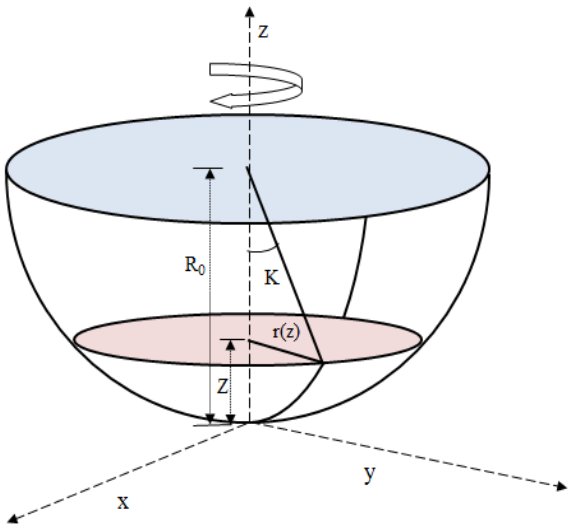

Figure 3 Geometry of ball end mill

Lag angle (Ψ) is the angle between the line which connects the cutting point to the tool tip on the x-y plane, and the tangent to the cutting edge at the tool tip. The lag angle can be expressed as follows: (Figure 3)

$$\Psi_j(z) = \frac{z}{R_0}\tan i_0 \tag{4}$$

Where i_0 is the helix angle which defines the twist of cutting edge(s).

Radial Immersion angle, $\Phi_j(z)$ define the angular position of a point on the cutting edge in the x-y plane measured from the +y axis. The radial immersion angle can be expressed as follows:

$$\Phi_j(z) = \theta + (j-1)\Phi_p - \Psi_j(z) \tag{5}$$

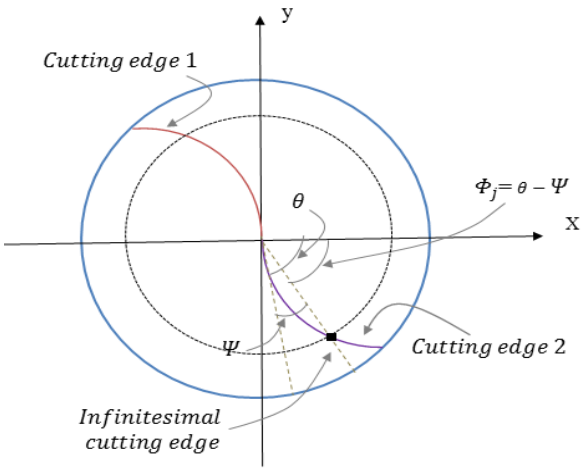

Figure 4 Geometry of ball end mill (Top view of chip element at rotation angle at θ)

Here Φ_p is the pitch angle between the preceding cutting edges. The pitch angle, depends on the total number of cutting edge on the tool and θ is the angular rotation of the tool.

$$\Phi_p = \frac{2\pi}{N_f}$$

From the above geometric parameters – axial distance from tool tip (Z), local radius $r(z)$, and radial immersion angle $\Phi(z)$, the discretized surface points of the tool in TCS are generated using the following equation 6. These discretized points are shown with the help of surface grid in figure 5. This grid is essentially the area swept by the cutting edge as the tool rotates about its axis.

$$\begin{aligned} xx_{tcs}(z) &= r(z) * \sin \Phi\,(z) \\ yy_{tcs}(z) &= r(z) * \cos \Phi(\mathrm{z}) \\ zz_{tcs}(z) &= z \end{aligned} \tag{6}$$

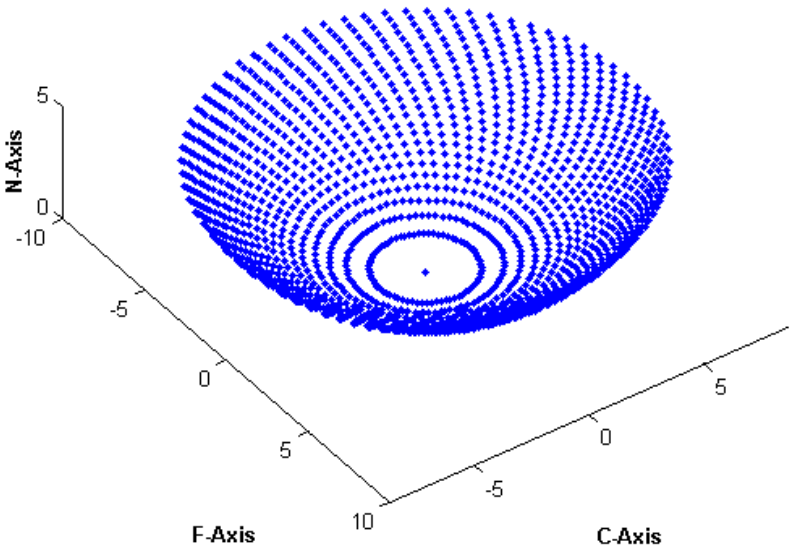

Figure 5 Discretised cutting points in FCN coordinate system

The density of the discretized surface points is controlled by defining angular incremental($d\theta$) and axial incremental (dz) values. Thus number of angular integration points (K) and axial integration points (L) are computed from equation 7 for a given ball end radius and 2π rotation. Generally, $\delta\theta$ is taken as 1° and δz is as taken as one-tenth of the cutting depth.

$$K_p = \frac{2\pi}{d\theta}$$
$$L_p = \frac{r}{dz} \tag{7}$$

2.1.3 Tool Orientation Parameters for 5-Axis Machining

In the case of 5-axis machining, the tool axis orientation is defined with the help of two angles. First is the lead angle (*lead*) which is the angular rotation of tool axis about the cross feed direction (C) with respect to the surface normal (N). Second is the tilt angle (*tilt*) which is the angular rotation of tool axis about the feed direction (F) with respect to the surface normal (N). The lead and tilt angles are used to transform the coordinates of the discretized surface points (as computed in equation 6) from FCN coordinate system to TCS .This is done using a transformation matrix T as shown in equation 8.

$$T = \begin{bmatrix} \cos(lead) & 0 & \sin(lead) \\ \sin(lead) * \sin(tilt) * & \cos(tilt) & -\sin(tilt) * \cos(lead) \\ -\cos(tilt) * \sin(lead) & \sin(tilt) * \sin(lead) & \cos(tilt) * \cos(lead) \end{bmatrix} \tag{8}$$

The transformation from FCN to TCS is achieved by first rotating the tool axis by the *tilt angle* in the NC plane. As a result the original FN plane gets rotated by the tilt angle about feed direction (F). This is followed by rotation of the tool axis by lead angle in the rotated FN plane.

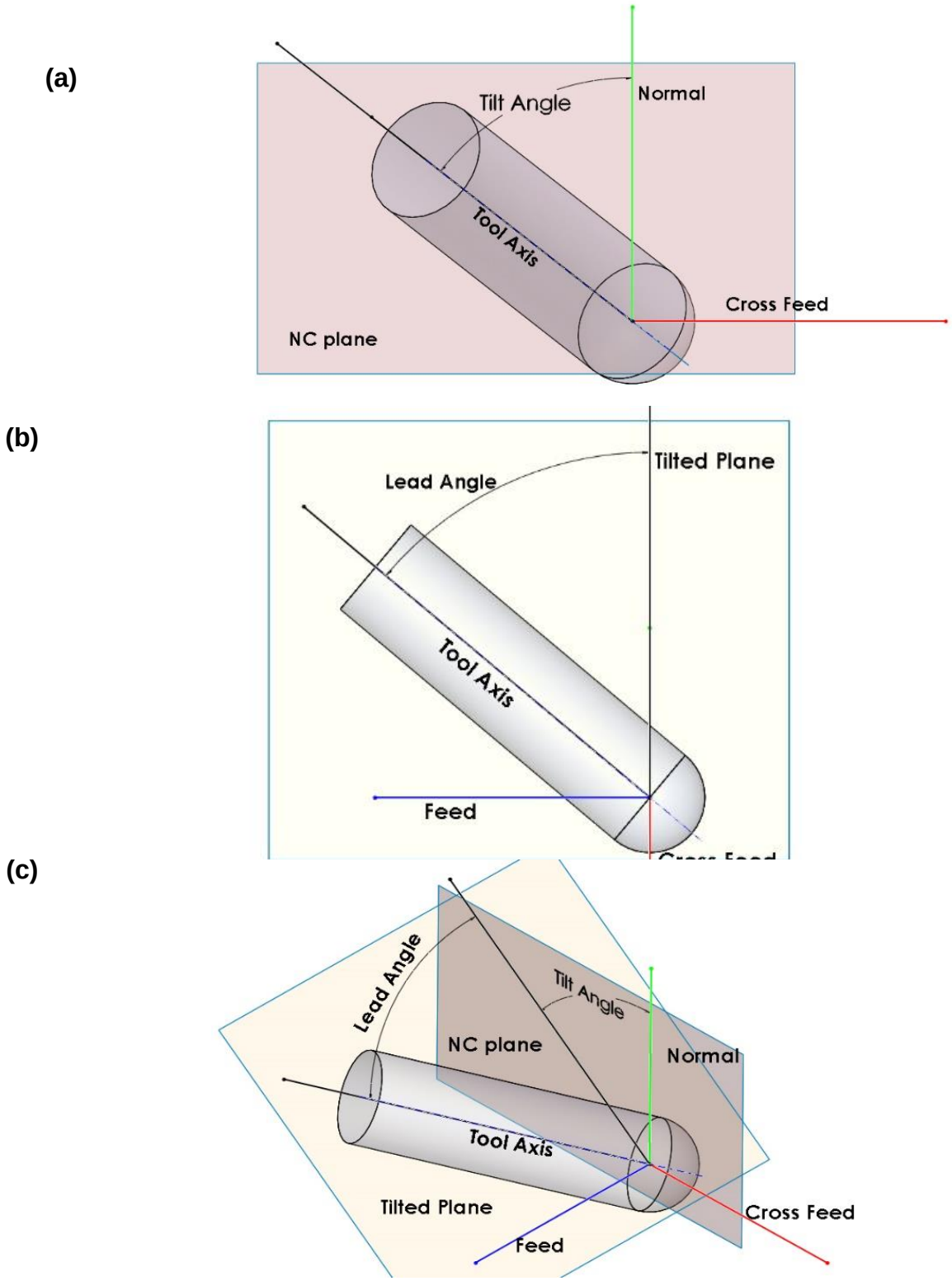

Figure 6 (a) Tilt angle define in NC plane, (b) Lead angle in tilted FN plane. (c) Rotated view of tool showing lead and tilt angle

2.1.4 Identification of Cutting Zone

Cutting zone is defined as portion of the tool in contact with the uncut material along the feed direction. The forces and torque exerted on the tool arise when the cutting edge(s) removes the uncut material present in this cutting zone.

This zone is modelled for a given cutting depth by identifying the set of discretized cutting points in FCN coordinate system which lie ahead of the NC plane along the positive feed direction. In order to identify this set of points, first the dot product of the feed vector with the position vectors of all the discretized cutting points is calculated. Then the points which have dot product greater than zero are identified as the cutting zone points as shown in equation 9. (Refer figure 8)

$$P(j,i) = \overrightarrow{feed} \cdot \overrightarrow{O_{new}X}(j,i)$$

$$\text{Cutting zone points} = P(j,i) > 0 \tag{9}$$

Where

$\overrightarrow{feed}$ is the feed vector which is user defined and

$\overrightarrow{O_{new}X}(j,i)$ is the position vectors of all the discretized cutting points with respect to lowest points of cutting tool in FCN coordinates system.

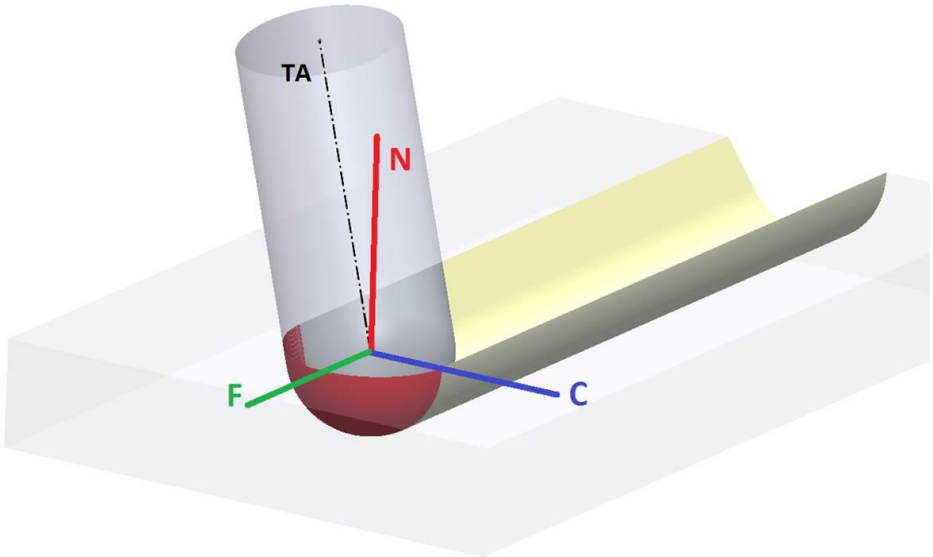

Figure 7 Cutting tool in FCN coordinate system

(a)

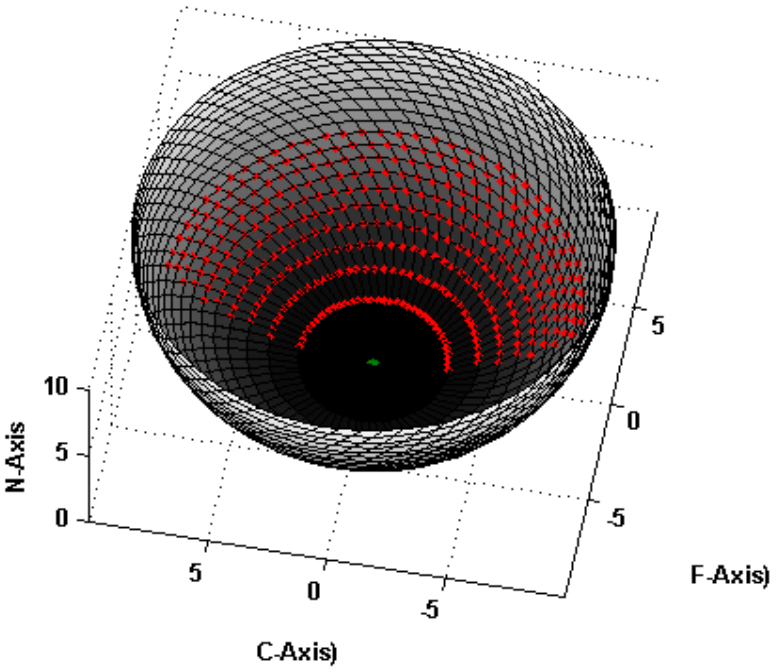

(b)

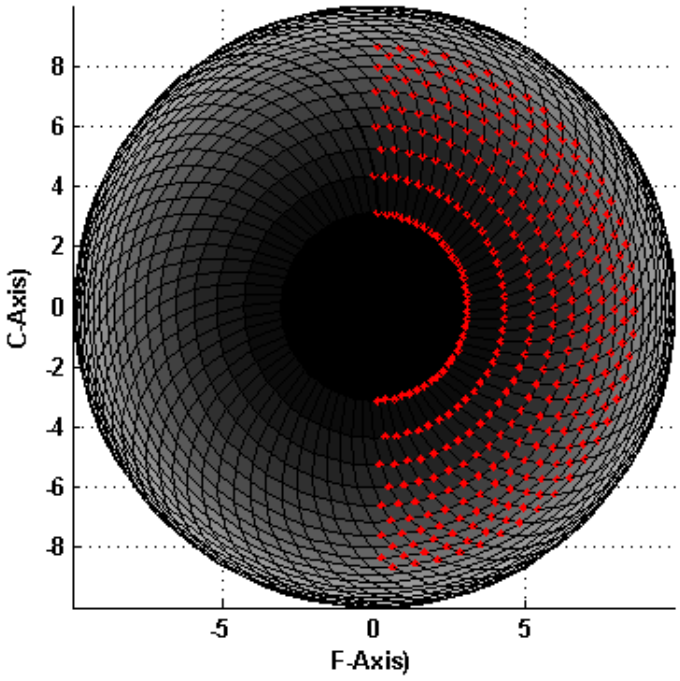

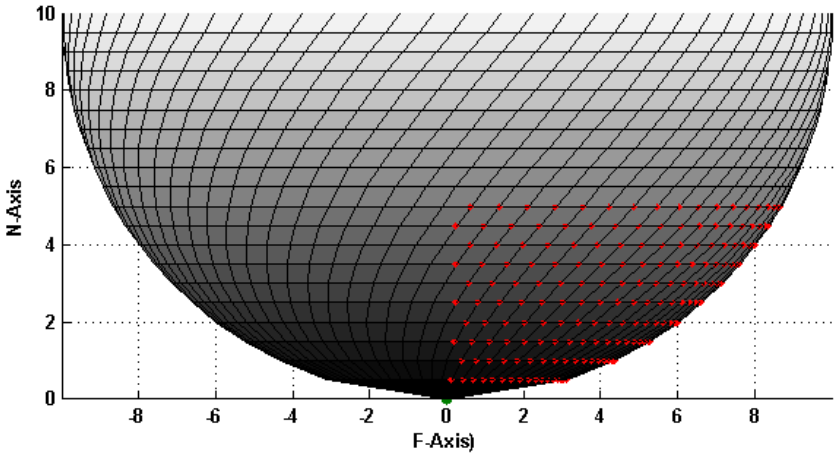

(c)

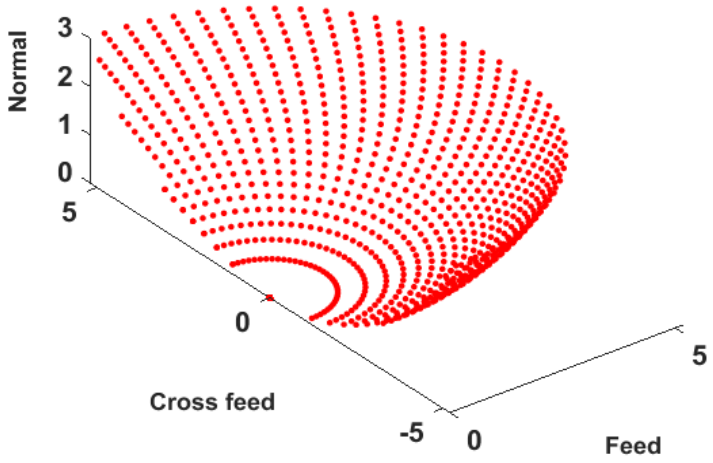

(d)

Figure 8 (a) Cutting zone points on cutting tool envelope.

(b) Cutting zone points in FC plane.

(c) Cutting zone points in FN plane.

(d) Discretised cutting zone points in FCN coordinate system.

2.2 Chip Dimension (Chip Volume)

During machining the material is removed from the workpiece in the form of chips. The forces generated on the tool are implicitly related to the morphology of these chips. Thus geometric parameters which define the morphology of the chips are required in order to compute the forces. The geometric parameters of the chips vary with respect to tool geometry (tool diameters, helix angle), machining process parameters (cutting feed and cutting depth) and the tool orientation (lead and tilt angle).There are three geometric parameters which are as follows:

- Chip thickness
- Chip width
- Chip length

The chip parameters are evaluated in a discrete manner by considering several infinitesimal cutting elements which form the cutting edge. A single element is formed by a line segment joining two discretized cutting points (as described in the previous section) which lie on the cutting edge.

Chip thickness is the thickness of the uncut material removed by the cutting edge in its normal direction. This is essentially the component of cutting feed in the direction normal to the cutting edge. It is a function of radial immersion angle (Φ), axial immersion angle (K) and feed (S_t) as shown in equation 10.

$$t_n(\Psi, \theta, \mathrm{K}) = S_t \, sin\, K \, sin\Phi \tag{10}$$

Where S_t is the feed per tooth

Chip width is defined as the projected length of an infinitesimal cutting edge in the direction of the cutting velocity. The nature of chip width depends on the tool rotation angle, axial immersion angle and depth of cut as shown in figure 9. It gradually increases from the cutting tool rotation of 0º to 90º and again reduces to minimum from 90º to 180º. The mathematical expression for chip width is shown in equation 11.

$$db = \frac{dz}{sinK} \tag{11}$$

Where dz is axial increment value along tool axis.

Chip length is defined as the Cartesian distance between two discretized cutting points which form the nodes of the infinitesimal cutting element. This is expressed mathematically as in equation 12.

$$ds = \sqrt{(\bar{X}\,(j+1,i) - \bar{X}(j,i))^2} \tag{12}$$

Where $\bar{X}(j+1,i)$ and $\bar{X}(j,i)$ represent the set of (x,y,z) coordinates of the two cutting points.

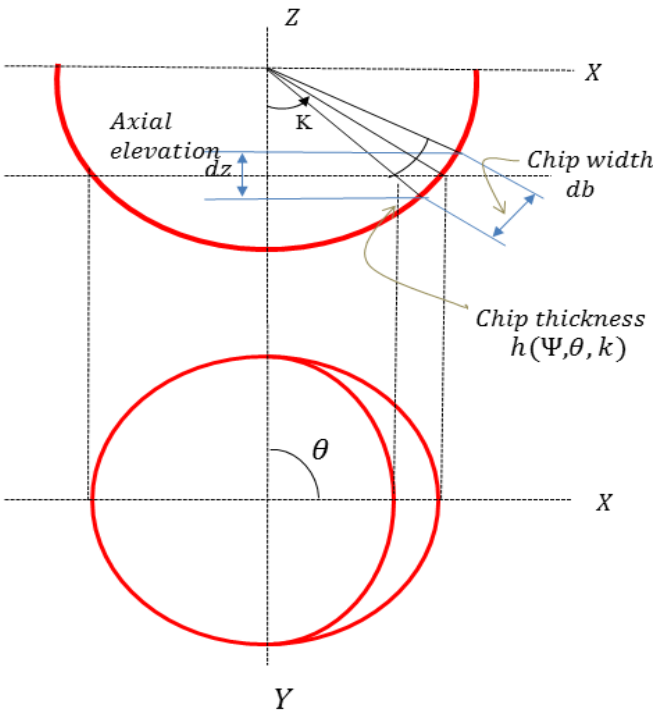

Figure 9 Chip geometric parameters (chip width and chip thickness)

2.3 Edge and Cutting Force Coefficients

As discussed in the section 2.1.2, the cutting edge is discretized into several infinitesimal cutting elements. These elements can be considered as a set of linear cutting edges undergoing oblique cutting with different/individual inclination angles. Hence the forces are computed for each of these elements using oblique cutting theory. Each elemental force has components acting in the radial, tangential and axial direction (in the local coordinate system).

In order to compute the above mentioned force components, two types of coefficients are required to be calculated in addition to the chip geometric parameters (Refer section 2.2). These are the edge force coefficients (K_e) and the cutting force coefficients (K_c) which are calculated for each of the three force components.

2.3.1 Edge Force Coefficients

Differential cutting forces are generated due to two processes—a primary process which includes shearing of the work material in the shear zone, and a secondary process which involves rubbing or ploughing at the cutting edge.

The edge force coefficient is evaluated from analyzing the secondary process which includes rubbing of the cutting edge on the uncut work material. This represents the rubbing force per unit length. This coefficient is obtained mechanistically for each of the three force components, i.e. along the tangential (K_{te}), radial (K_{re}) and axial (K_{ae}) direction, by performing several orthogonal cutting experiments for varying tool geometry and process parameters. However, it has been observed that the edge coefficient does not vary significantly with cutting speeds, rake angles for a particular work material.

For titanium (Ti_6Al_4V) the values of the edge coefficients are

$$K_{te} = 24 \text{ N/mm}$$
$$K_{re} = 43 \text{ N/mm}$$
$$K_{ae} = 0 \text{ N/mm}$$

Since K_{ae} value is usually small and taken as zero.

2.3.2 Cutting Force Coefficients

Evaluation of cutting force coefficients involves analysis of the primary cutting process which is essentially the shearing of the work material in the shear zone. This represents the cutting force per unit chip cross-sectional area. Just as in the case of edge coefficients, cutting force coefficients are evaluated for each of the three force components i.e. along the tangential (K_{tc}), radial (K_{rc}) and axial (K_{ac}) directions. They are calculated using the orthogonal cutting database and oblique cutting model transformation.

Orthogonal Cutting Database

The orthogonal cutting database essentially provides an empirical relationship between a given set of machining process parameters (feed and rake angle) and the material shearing parameters such as friction angle and shear angle. (Refer Table 1)

Table 1 Input and output of orthogonal Cutting database (OCD)

Input to the OCD (Machining parameters)	Output from OCD (Material shearing parameters)
• Cutting feed • Rake angle	• Chip compression ratio/cutting ratio (r), • Shear stress (τ), • Friction angle (β). • Shear angle (φ)

Shear angle (φ) can be estimated as follows:

$$tan\varphi = \frac{r\cos\alpha}{1 - r_t \sin\alpha}$$

The empirical relationship obtained from the OCD is summarized in Table 2. It is observed that the shear stress (τ) does not vary significantly with either the rake angle or the cutting speeds. Hence it is taken as a constant which is 613 MPA for a given

material (Ti_6Al_4V). The friction angle (β) is expressed as a function of the rake angle (α), while the cutting ratio (r) is a function of the uncut chip thickness. However, this relationship is true only for titanium (Ti_6Al_4V), and other materials may exhibit different relationships.

Table 2 Orthogonal Cutting database (OCD)

τ = 613 MPA β = 19.1+0.29α
$r_{=}r_0 t^a$ r_0=1.755-0.228α a =0.331-0.0028α

Oblique Cutting Mechanics

As discussed in section 2.1.2, the cutting edge of the tool is discretized into several infinitesimal cutting elements. These elements are essentially a set of discretized cutting edges undergoing oblique cutting. Every cutting element is orientated at an inclination angle with respect to cutting velocity. Subsequently, Merchant's theory for oblique cutting is used to resolve the resultant cutting force on the shear plane into three mutually perpendicular components as follows:

- Tangential force (F_t), acting along the direction of cutting velocity.
- Feed force (F_f) acting along the direction of uncut chip thickness or in other words, in the direction of cutting feed.
- Radial force (F_r) acting along the radial direction (perpendicular to both tangential and feed).

The above forces are expressed mathematically as follows:

$$F_t = \frac{\tau bt}{sin\varphi_n}\frac{\cos(\beta_n - \alpha_n) + tan\eta_c \sin\beta_n \tan i}{c}$$

$$F_f = \frac{\tau bt}{sin\varphi_n cosi}\frac{\sin(\beta_n - \alpha_n)}{c} \quad (13)$$

$$F_r = \frac{\tau bt}{sin\varphi_n}\frac{\cos(\beta_n - \alpha_n)\, tani - \sin\eta_c \tan\beta_n}{c}$$

Where

$$c = \sqrt{cos^2(\varphi_n + \beta_n - \alpha_n) + tan^2\eta_c\, sin^2\beta_n}$$

- Normal friction angle (β_n) is obtained as

$$tan\beta_n = tan\beta \cos\eta_c$$

Where β is the average friction angle at the rake face in orthogonal cutting.

- Normal rake angles (α_n)
- Chip flow angle (η_c)
- Normal shear angle (φ_n) expressed as:

$$tan\varphi_n = \frac{r_t \cos\alpha_n}{1 - r_t \sin\alpha_n}$$

- r_t is the equivalent chip thickness ratio in oblique cutting and is obtained using orthogonal chip thickness ratio r, as follows:

$$r_t = r\frac{\cos\eta_c}{\cos i}$$

From the force equation the cutting force coefficients acting in the tangential, feed and radial directions as follows:

$$K_t = \frac{\tau}{sin\varphi_n}\frac{\cos(\beta_n - \alpha_n) + tan\eta_c \sin\beta_n \tan i}{c} \quad (14)$$

$$K_f = \frac{\tau}{sin\varphi_n cosi} \frac{\sin(\beta_n - \alpha_n)}{c}$$

$$K_r = \frac{\tau}{sin\varphi_n} \frac{\cos(\beta_n - \alpha_n)\, tani - \sin\eta_c \tan\beta_n}{c}$$

The following assumptions are made in order to transform orthogonal cutting mechanics to oblique cutting process:

- Normal rake angle (α_n) and normal shear angle (φ_n) in oblique cutting is same as the orthogonal rake angle (α_0) and orthogonal shear angle (φ_0) respectively:

$$\alpha_n = \alpha_0$$

$$\varphi_n = \varphi_0$$

- Friction angle and shear stress are same in both orthogonal and oblique cutting for a given speed, chip load and tool workpiece pair:

$$\beta_n = \beta$$

$$\tau_s = \tau$$

- Chip flow angle (η_c) is approximated by the local inclination angle:

$$\eta_c = i$$

However, the oblique cutting force components, i.e. dF_t, dF_f and dF_r are equivalent to the mutually perpendicular forces in the ball-end cutter's local coordinate system which are along the tangential, radial and axial directions. Hence the force coefficients K_t, K_f and K_r are respectively equivalent to the cutting force coefficients K_{tc}, K_{rc} and K_{ac} in the local coordinate system.

$$K_{tc} = \frac{\tau}{sin\varphi_n} \frac{\cos(\beta_n - \alpha_n) + tan\eta_c \sin\beta_n \tan i}{c}$$

$$K_{rc} = \frac{\tau}{sin\varphi_n} \frac{\sin(\beta_n - \alpha_n)}{c} \quad (15)$$

$$K_{ac} = \frac{\tau}{sin\varphi_n} \frac{\cos\ (\beta_n - \alpha_n)\, tani - \sin\eta_c \tan\beta_n}{c}$$

2.4 Force and Torque Computation

The computation of forces and torque acting on the tool first begins with the identification and separation of the discretized surface points which lie in the cutting zone, and those which lie outside of it. The identification of the points lying in the cutting zone is described in section 2.1.4. Once the points have been identified and separated, only the points lying in the cutting zone are used for the calculation of chip and cutting edge geometric parameters, which eventually are used for the computation of cutting forces. For the points outside the cutting zone the above parameters, forces and torque are nullified.

2.4.1 Logical Matrix

A logical matrix (LG) consisting of 1s and 0s is defined in order to identify and separate all those discretized surface points which lie in the cutting zone. An element in LG with value 1 indicates that the corresponding point lies within the cutting zone. On the other hand, an element with value 0 indicates that the corresponding point lies outside the cutting zone.

This logical matrix LG is used as a multiplication factor in calculations of cutting edge geometric parameters (i.e. axial immersion angle K, radial immersion angle Φ) and chip geometric parameters (i.e. chip thickness t_n , chip width db, chip length ds). As a result all those points lying in the cutting zone have a specific and definite value for the above parameters, and for the points outside the cutting zone the same parameters are set to zero.

Subsequently, only the points in the cutting zone return a specific value for the forces and torque, and the points outside the zone return no value or numerically zero. This physically implies that the forces are generated in the tool only when the cutting edge(s) are inside the cutting zone.

2.4.2 Force Mechanistic Equation

As described in section 2.3.1, the cutting forces in the tool arise as a result of shearing the of the work material (primary process) and due to the ploughing or rubbing at the cutting edge (secondary process).

The edge force coefficients $K_{te,}\ K_{re,}\ K_{ae}$ (section 2.3.1) and the cutting force coefficients $K_{tc,}\ K_{rc,}\ K_{ac}$ are determined using oblique cutting mechanics (section 2.3.2). Subsequently the differential cutting forces for a given cutting edge j in the tangential, radial and axial directions for a particular cutting element are expressed as follows: (Figure 10)

$$\begin{aligned} dF_t(\theta,z) &= K_{te}ds_c + K_{tc}t_{nc}(\Psi,\theta,K)db_c \\ dF_r(\theta,z) &= K_{re}ds_c + K_{rc}t_{nc}(\Psi,\theta,K)db_c \\ dF_a(\theta,z) &= K_{ae}ds_c + K_{ac}t_{nc}(\Psi,\theta,K)db_c \end{aligned} \tag{16}$$

Where

$$\begin{aligned} ds_c &= LG \cdot ds \\ t_{nc} &= LG \cdot t_n \\ db_c &= LG \cdot db \end{aligned} \tag{17}$$

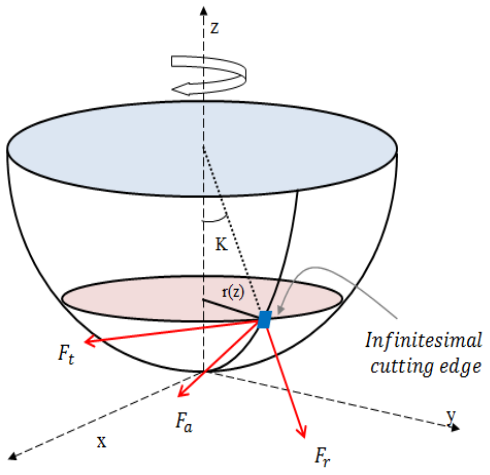

Figure 10 Differential forces in local coordinate system acting on infinitesimal cutting edge

In the above set of equations, the differential forces (dF_t, dF_r, dF_a) are computed in the tangential, radial and axial directions of the tool for a particular angular rotation (θ) and axial elevation (z) along the tool axis. The product of edge force coefficients ($K_{te,}\ K_{re,}\ K_{ae}$), which represent the force per unit chip length, with the length of the cutting element ds gives the edge/ploughing component of the resultant force.

Similarly, the product of cutting force coefficients ($K_{tc,}\ K_{rc,}\ K_{ac}$), which represent the force per unit chip area, with the chip cross-sectional area ($t_n \cdot db$) gives the cutting/shearing component of the resultant force. By including LG in the above computation, the forces are evaluated only in the cutting zone and get nullified in the remaining portion of the tool.

Note that equation 17, ds, t_n and db are respectively the matrices consisting of chip length, chip thickness and chip width of all cutting elements formed using the discretized surface points of the tool (i.e. all points inside and outside of the cutting zone). Further, equation 17 is actually an element wise matrix multiplication operation, in which a particular element in the first matrix is multiplied with the element having the same index in the second matrix only.

2.4.3 Forces Transformation

The above differential forces $dF_t, dF_r, dF_a,$ which are in the elemental local coordinate system, can be transformed to the tool coordinate system TCS (xyz) using a transformation matrix (A). This is expressed as follows:

$$\begin{Bmatrix} dF_x \\ dF_y \\ dF_z \end{Bmatrix}_{TCS} = [A] \begin{Bmatrix} dF_t \\ dF_r \\ dF_a \end{Bmatrix}_{LCS} \tag{18}$$

Where

$$A = \begin{bmatrix} -\sin(K)\sin(\Phi) & -\cos(\Phi) & -\cos(K)\sin(\Phi) \\ -\sin(K)\cos(\Phi) & \sin(\Phi) & -\cos(K)\cos(\Phi) \\ -\cos(K) & 0 & -\sin(K) \end{bmatrix}$$

And K is the axial immersion angle and Φ is the radial immersion angle. (Refer section 2.1.2)

Further, the differential torque acting on each cutting element can also be determined as the product of the instantaneous radius of that element with the tangential cutting force acting on it.

$$dT_{TCS} = r(z) \cdot dF_t \tag{19}$$

The total cutting forces acting on the tool for a given angular rotation (θ) in TCS are then determined by summation of the differential forces for all the cutting elements. This is expressed as follows:

$$F_x(\theta) = \sum_{j=1}^{n}\sum_{i=1}^{m} dF_x(\theta, z)$$

$$F_y(\theta) = \sum_{j=1}^{n}\sum_{i=1}^{m} dF_y(\theta, z) \tag{20}$$

$$F_z(\theta) = \sum_{j=1}^{n}\sum_{i=1}^{m} dF_z\,(\theta, z)$$

Similarly, the total torque acting on the tool in TCS is expressed as follows:

$$T_{TCS}(\theta) = \sum_{j=1}^{n}\sum_{i=1}^{m} dT_{TCS}\,(\theta, z) \tag{21}$$

Where n is total number of cutting edge(s) in the tool and m is total number of axial elevations (z) along the tool axis.

The above cutting forces in TCS can also be transformed to forces in FCN coordinate system using the transformation matrix T as follows:

$$\begin{Bmatrix} F_F \\ F_C \\ F_N \end{Bmatrix}_{FCN} = [T] \begin{Bmatrix} F_x \\ F_y \\ F_z \end{Bmatrix}_{TCS} \tag{22}$$

Where

$$T = \begin{bmatrix} \cos(lead) & 0 & \sin(lead) \\ \sin(lead) * \sin(tilt) * & \cos(tilt) & -\sin(tilt) * \cos(lead) \\ -\cos(tilt) * \sin(lead) & \sin(tilt) * \sin(lead) & \cos(tilt) * \cos(lead) \end{bmatrix}$$

Note: All the forces are modelled with respect to tool rotation. Hence the resulting force and torque data and plots are obtained as a function of tool rotation.

2.5 Results and Validation

In order to verify, the simulated data obtained from the model was compared with both published literature data as well as experiments performed on 3-axis milling operation. Several model simulations were performed by varying basic process parameters such as cutting depth, feed rate, spindle speed and tool orientation parameters (lead and tilt).

The model simulation were performed considering the helical ball end mill as the cutting tool, and titanium alloy (Ti6Al4V) as the workpiece material undergoing slotting operation.

2.5.1 3-Axis Machining Simulation

The Model was validated for two different cases of slot milling operations obtained from the published literature. The force data was plotted as a function of tool rotation and then a visual comparison was done with the published plots.

The input data and the resulting simulated force and torque output for the different cases are as follows:

Case 1

Table 3 Inputs for case 1 (from literature, 3-axis)

Tool geometric parameters	Diameter, D=19.01 mm Helix angle, i_0=30° Rake angle, α=0° Number of cutting edges, N_f =1
Machining process parameters	Spindle speed, n =269 rpm Table feed, S_t=13.6652 mm/min Depth of cot, $doc = 6.35$ mm
Tool orientation parameters	Lead angle, $lead = 0°$ Tilt angle, $tilt = 0°$

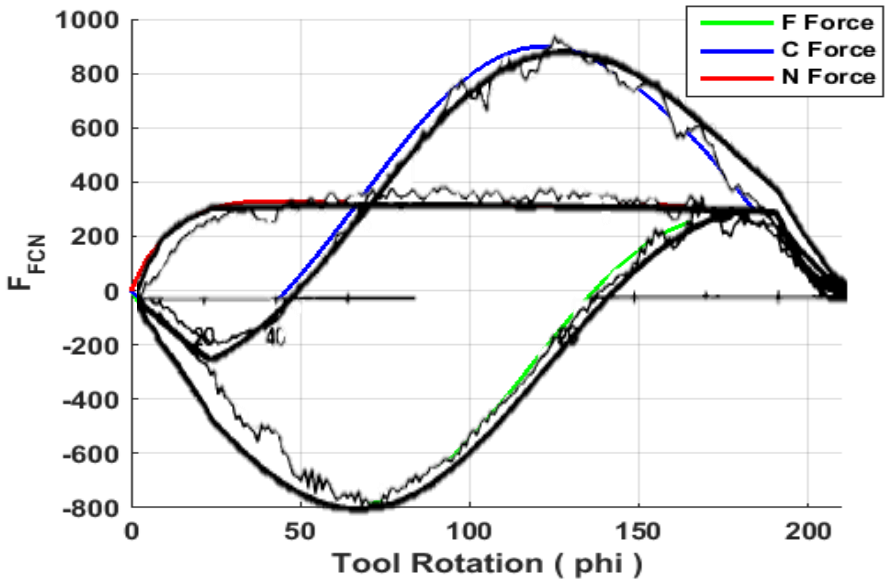

Figure 11 Comparision of simulated cutting force results with published results.

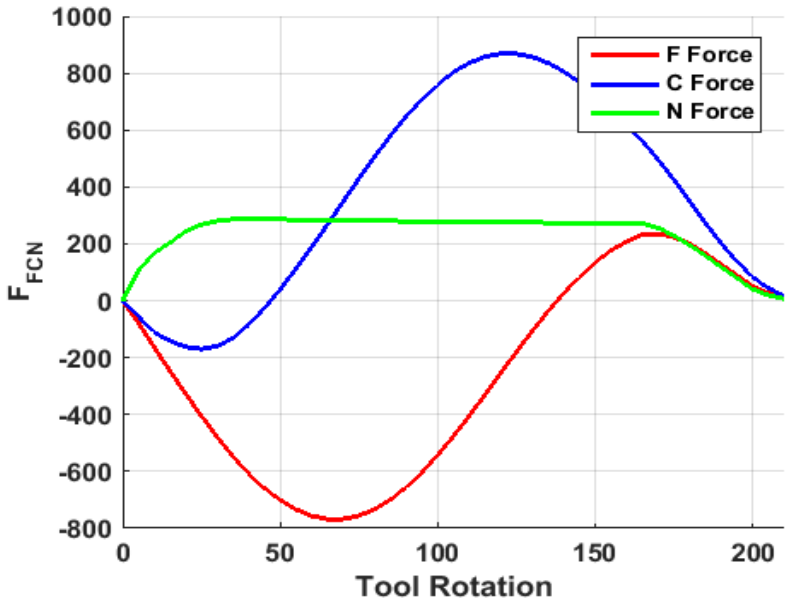

Figure 12 Cuttng forces in FCN corodinate system for Table 3 inputs.

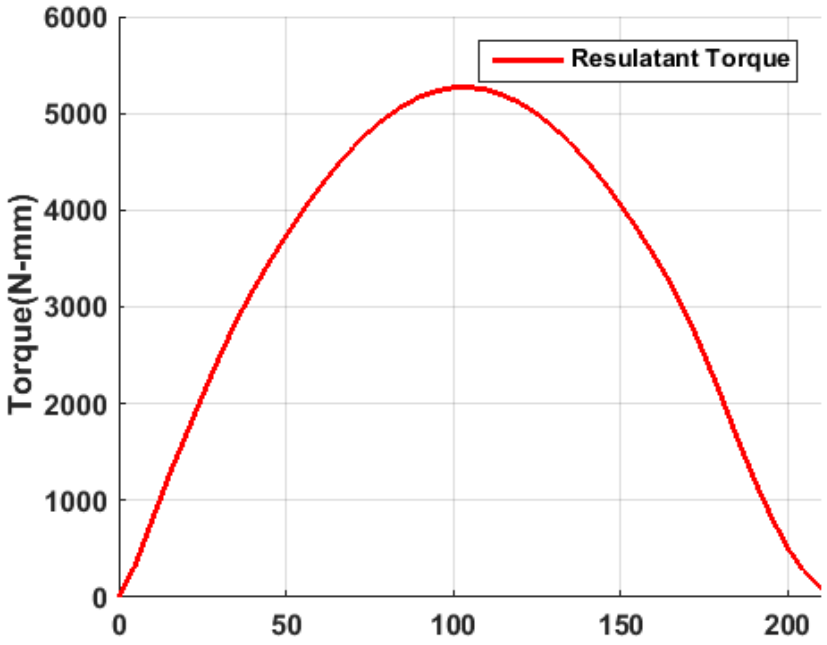

Figure 13 Torque varation in TCS for Table 3 inputs

As lead and tilt angles are zero (i.e. for 3-axis milling process), the Feed (F), Cross-feed (C) and Normal (N) forces correspond to the forces in X, Y and Z directions respectively.

As the tool begins to rotate from 0° through 180°, the chip thickness varies from minimum at the beginning i.e. when the cutting edge enters the cutting zone; reaches a maximum thickness mid-way through the rotation (approximately 120° as evident in the figure 12); and then minimum again as the cutting edge exits the cutting zone. It is observed that the Cross-feed force (C) reaches a maximum value where the chip thickness is maximum. This is due to the fact that the cross-feed force vector is normal to chip thickness direction. Further the Feed force (F) is minimum where the Cross-feed force (C) is maximum. (Why-need explanation)

Case 2

Table 4 Inputs for case 2 (from literature, 3-axis)

Tool geometric parameters	Diameter, D=19.01 mm Helix angle, i_0=30° Rake angle, α=0° Number of cutting edges, N_f =1
Machining process parameters	Spindle speed, n =269 rpm Table feed, S_t=13.6652 mm/min Depth of cot, $doc = 1.27$ mm
Tool orientation parameters	Lead angle, $lead = 0°$ Tilt angle, $tilt = 0°$

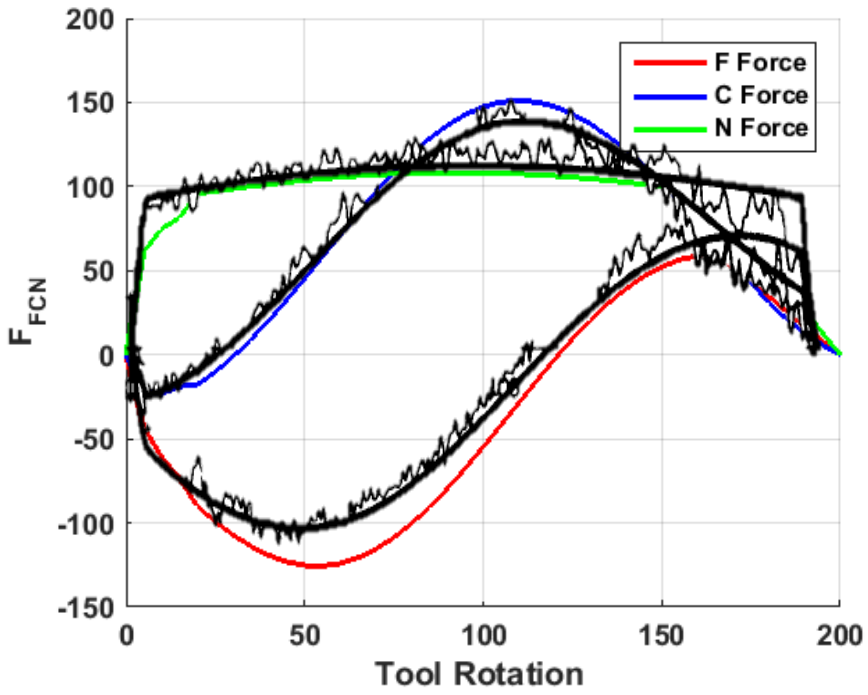

Figure 14 Comparision of simulated cutting force results with published results.

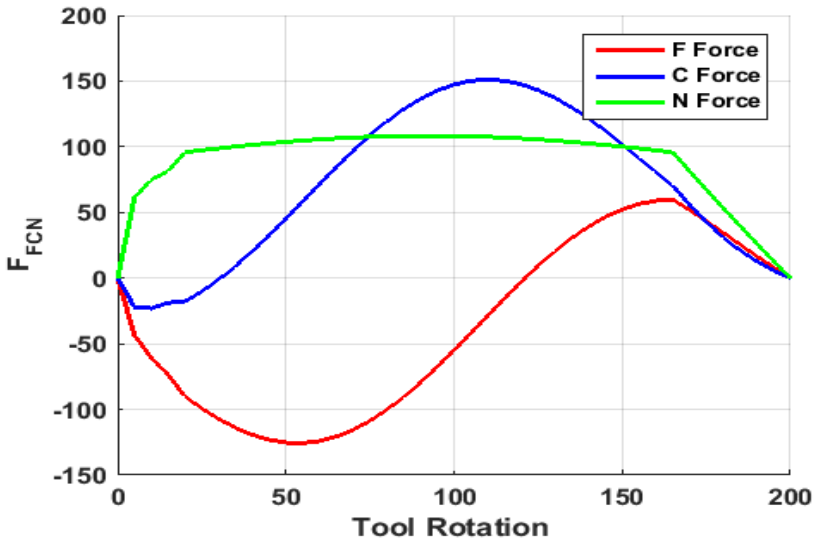

Figure 15 Cuttng forces in FCN corodinate system for Table 4 input**s.**

Figure 16 Torque varation in TCS for Table 4 inputs.

Case 3

Table 5 Inputs for case 3 (from literature, 3-axis)

Tool geometric parameters	Diameter, D=19.01 mm Helix angle, i_0=30° Rake angle, α=0° Number of cutting edges, N_f =1
Machining process parameters	Spindle speed, n =269 rpm Table feed, S_t=13.6652 mm/min Depth of cot, $doc = 1.27$ mm
Tool orientation parameters	Lead angle, $lead = 0°$ Tilt angle, $tilt = 0°$

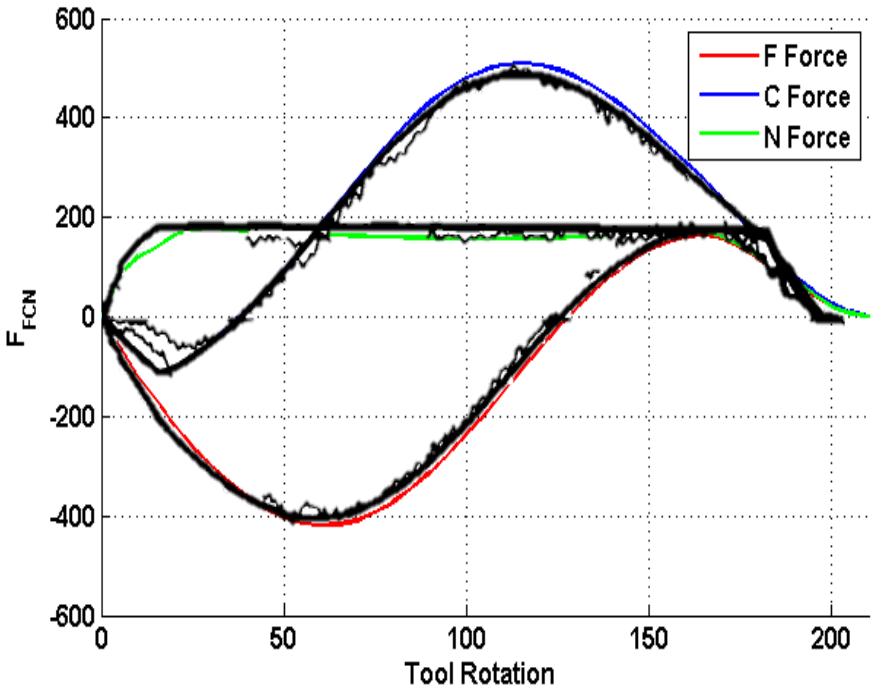

Figure 17 Comparision of simulated cutting force results with published results.

2.5.2 5-Axis Machining Simulation

Case 1

Table 6 Inputs for case 1 (from literature, 5-axis)

Tool geometric parameters	Diameter, D=12 mm Helix angle, i_0=30° Rake angle, α=8° Number of cutting edges, N_f =2
Machining process parameters	Spindle speed, n =500rpm Table feed, S_t=100 mm/min Depth of cot, $doc = 1.5$ mm
Tool orientation parameters	Lead angle, $lead = 30°$ Tilt angle, $tilt = 30°$

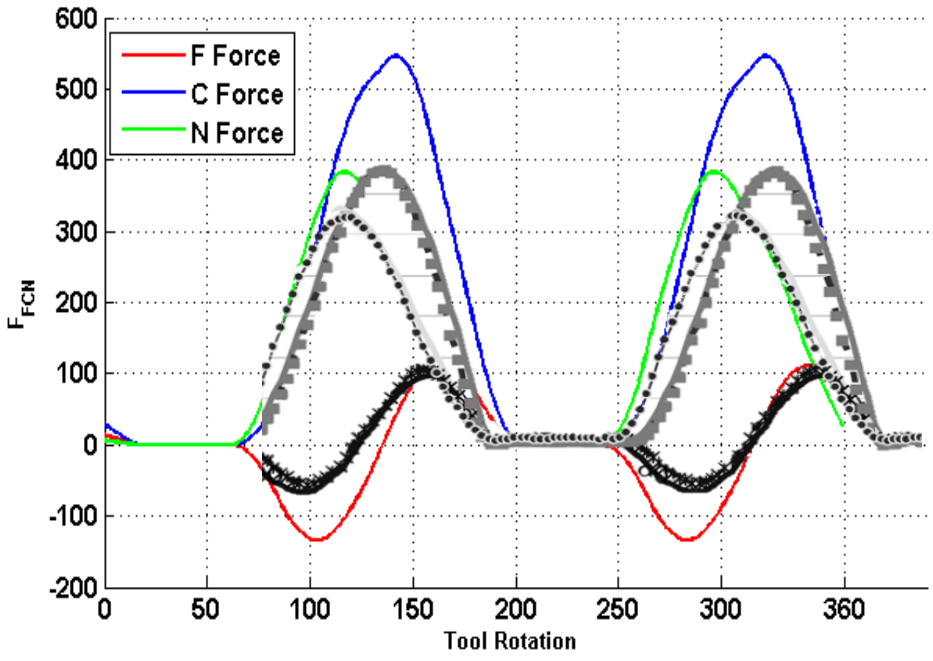

Figure 18 Comparision of simulated cutting force results with published results.

Case 2

Table 7 Inputs for case 2 (from literature, 5-axis)

Tool geometric parameters	Diameter, D=12 mm Helix angle, i_0=30° Rake angle, α=8° Number of cutting edges, N_f =2
Machining process parameters	Spindle speed, n =3000rpm Table feed, S_t=600 mm/min Depth of cot, $doc = 1.5$ mm
Tool orientation parameters	Lead angle, $lead = 10°$ Tilt angle, $tilt = -15°$

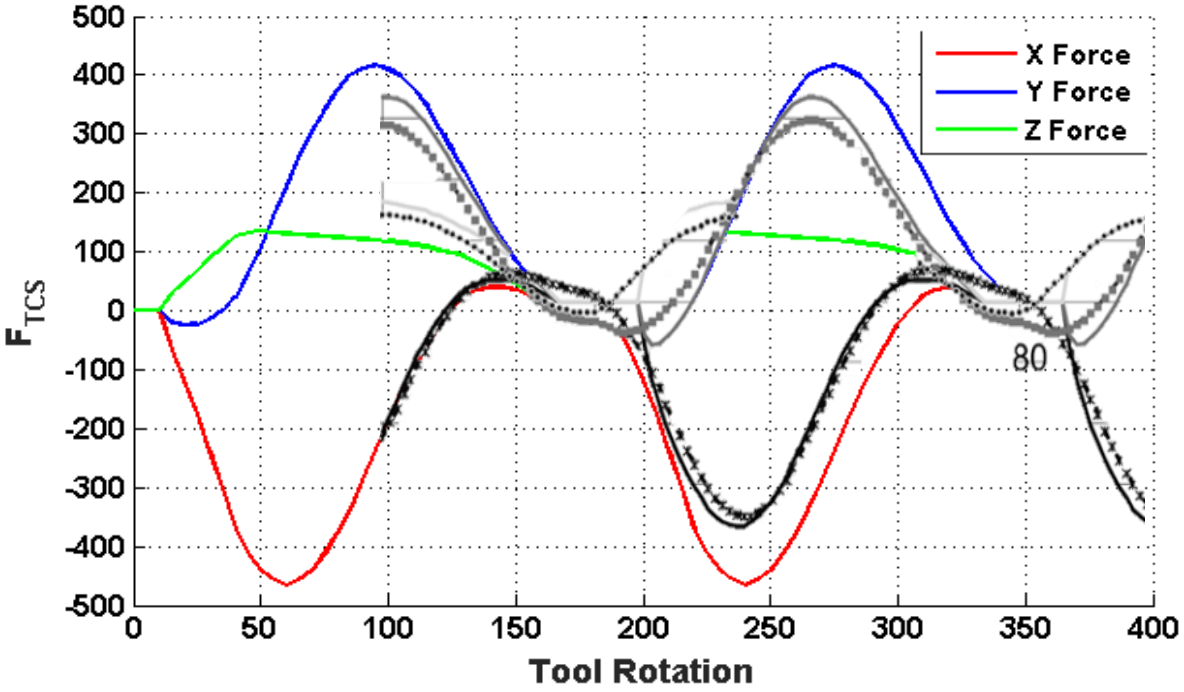

Figure 19 Comparision of simulated cutting force results with published results.

2.5.3 Experimental Verification

Case 1

Table 8 Inputs for case 1 (Experimental, 3-axis)

Tool geometric parameters	Diameter, D=20 mm Helix angle, i_0=40° Rake angle, α=10.5° Number of cutting edges, N_f =2
Machining process parameters	Spindle speed, n =500rpm Table feed, S_t=100 mm/min Depth of cut, $\boldsymbol{doc = 1\ mm}$
Tool orientation parameters	Lead angle, $lead = 0°$ Tilt angle, $tilt = 0°$

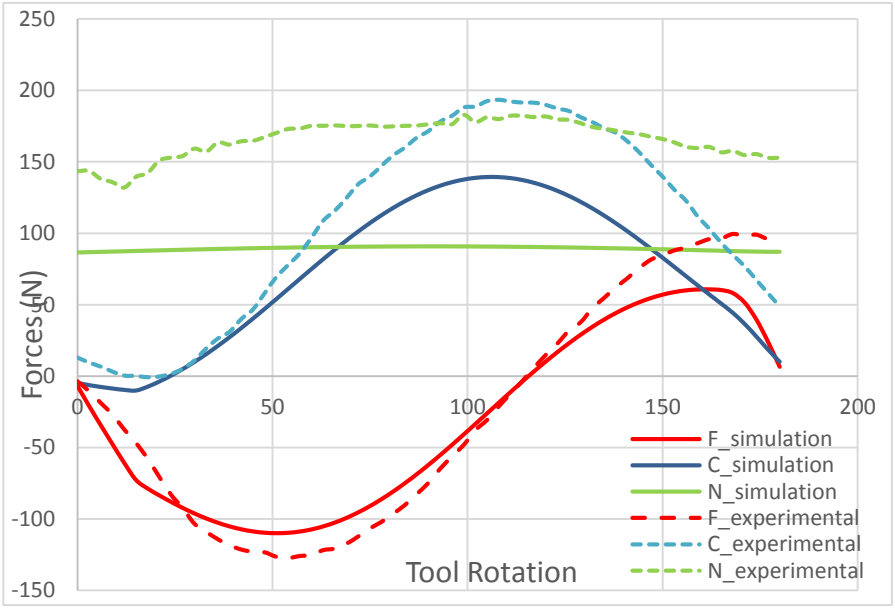

Figure 20 Simulated results verification with experimental results for case 1

Case 2

Table 9 Inputs for case 2 (Experimental, 3-axis)

Tool geometric parameters	Diameter, D=20 mm Helix angle, i_0=40° Rake angle, α=10.5° Number of cutting edges, N_f =2
Machining process parameters	Spindle speed, n =500rpm Table feed, S_t=100 mm/min Depth of cut, $\boldsymbol{doc = 1\ mm}$
Tool orientation parameters	Lead angle, $lead = 0°$ Tilt angle, $tilt = 0°$

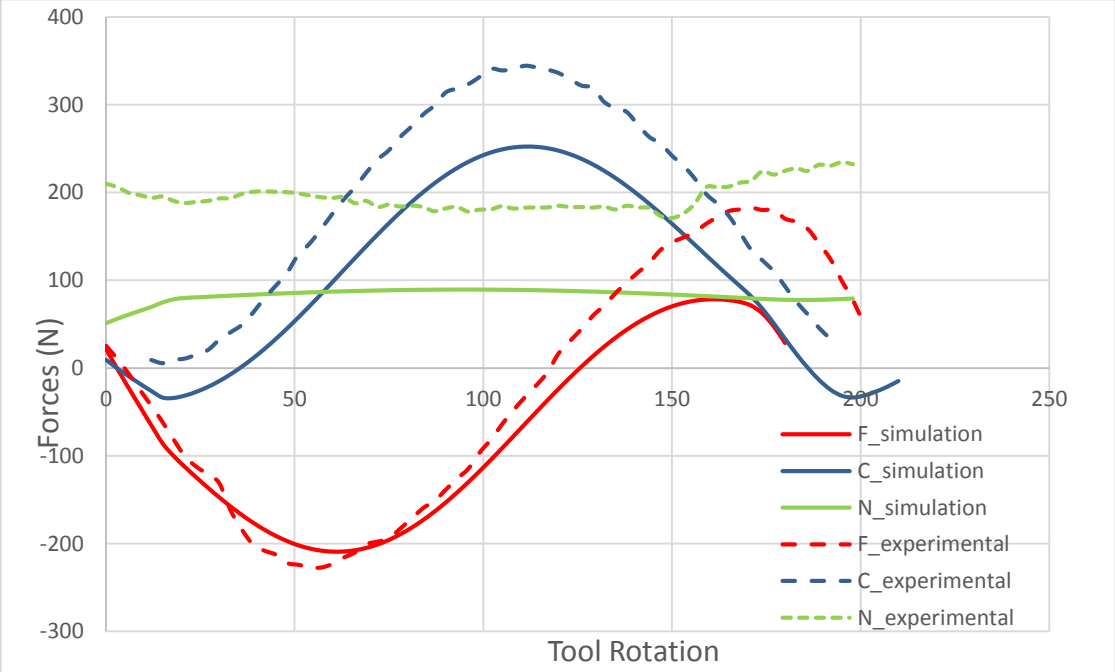

Figure 21 Simulated results verification with experimental results for case 2

Case 3

Table 10 Inputs for case 3 (Experimental, 3-axis)

Tool geometric parameters	Diameter, D=20 mm Helix angle, i_0=40° Rake angle, α=10.5° Number of cutting edges, N_f =2
Machining process parameters	Spindle speed, n =500rpm Table feed, S_t=100 mm/min Depth of cut, $\boldsymbol{doc = 1.5\ mm}$
Tool orientation parameters	Lead angle, $lead = 0°$ Tilt angle, $tilt = 0°$

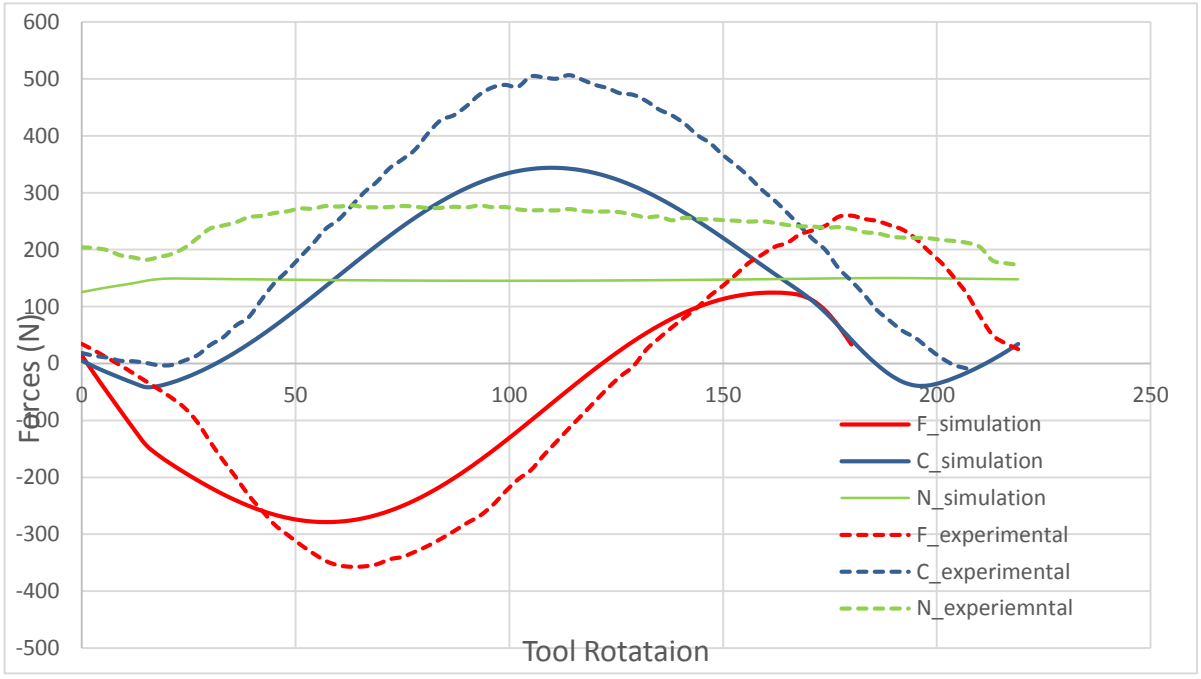

Figure 22 Simulated results verification with experimental results for case 3

2.6 Milling Process Simulator (MPS)

Milling Process Simulator (MPS) is a MATLAB based program which is developed for modelling and simulation of multi-axis milling operations using ball end mill as the cutting tool. With MPS, the user can predict the variation in cutting forces and torque acting on the tool during slot milling operations.

In order to run MPS, the user has to specify several geometry and process related inputs such as tool diameter, helix and rake angles, spindle speed, table feed, depth of cut, lead and tilt angles. A snapshot of the MPS user interface is shown in Figure 23 below.

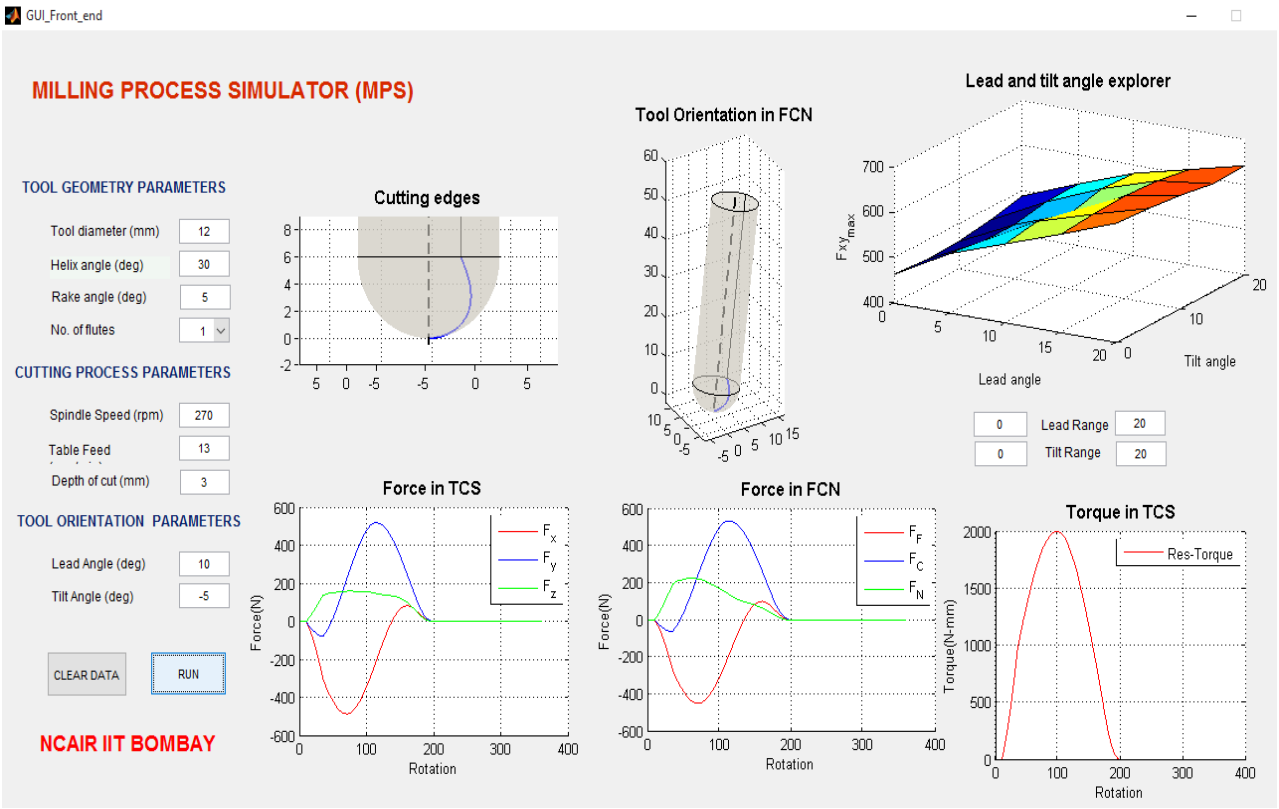

Figure 23 Graphical user interface of Milling Process Simulator (MPS)

The MPS has the following modules:

2.6.1 Pre-Processor Module

In this module the user inputs the following geometry and process parameters for which the forces and torques are to be predicted:

- Tool Geometry Parameters—Diameter (D), helix angle(i_0), rake angle (α) and number of cutting flutes(N_f).
- Cutting Process parameters—spindle speed(n), feed (S_t), and depth of cut (doc).
- Tool orientation parameters—Lead angle ($lead$), tilt angle ($tilt$). The user also needs to provide a minimum to maximum range for these angles.

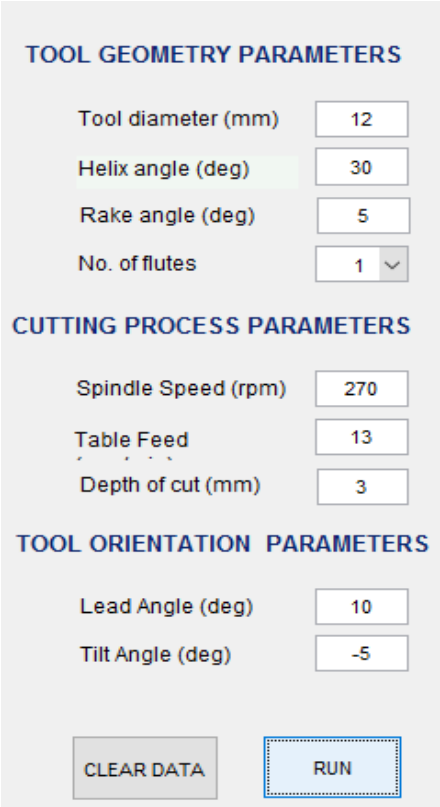

Figure 24 User defined inputs to MPS

2.6.2 Processor/modeler Module

The input data from the *Pre-processor* module is used internally to run several sections of the force model. Following internal computations are performed sequentially using the input data:

- **Geometric modelling of cutting edge(s):**
  Using the diameter (D) and helix angle(i_0), the axial distance from the tool tip (Z), Local radius($r(z)$), axial immersion angle (K), lag angle (Ψ) and radial immersion angle (Φ) are computed. (Refer section 2.1.2)
- **Generation of discretized surface points:**
  The ball end mill surface is discretized into several infinitesimal cutting points in TCS. The density of the discretized points is controlled using angular($d\theta$) and axial increment (dz) values. (Refer section 2.1.2)

- **Transformation of discretized surface points from TCS to FCN:**
  Using the Lead and Tilt angle values specified in the input the discretized surface points are transformed from TCS to FCN coordinate system using the transformation matrix. (Refer section 2.1.3)
- **Identification of cutting zone/cutting zone points:**
  Using the *Cutting Depth* value as the input, the discretized surface points (defined in FCN coordinate systems) which lie in the cutting zone (along the Feed direction and ahead of the C-N plane) are identified and separated. (Refer section 2.1.4)
- **Computation chip geometrical parameters:**
  Based on the input machining parameter values (*Feed rate and cutting depth*) the Chip geometrical parameters (chip thickness(t_n), chip width(db), chip length (ds)) are computed for the cutting zone points identified above. (Refer section 2.2)
- **Calculation of cutting force coefficients:**
  In this step, the cutting force coefficients are computed for all three force component directions, i.e. along the tangential (K_{tc}), radial (K_{rc}) and axial (K_{ac}) directions. These coefficients are calculated using the orthogonal cutting database and oblique cutting model transformation. (Refer section 2.3.2)
- **Computation of differential forces on each infinitesimal edges in LCS:**
  Using the cutting force coefficients and chip geometric parameters obtained from the previous steps, the differential forces (dF_t, dF_f, dF_r) acting on each infinitesimal cutting edge along the radial, tangential and axial directions are computed. Using dF_t and the instantaneous radius of the tool, the differential torque acting for individual cutting elements is calculated. (Refer section 2.4.2)
- **Transformation of differential forces to TCS:**
  The differential forces dF_t, dF_r, dF_a obtained above are transformed to tool coordinate system TCS. The total cutting forces on the tool in TCS are then found by the summation of all the differential forces for all the cutting elements. The differential torque values are also summed to give the total torque acting on the tool in TCS. (Refer section 2.4.3)

- **Transformation of forces from TCS to FCN coordinate system:**
  The previously computed cutting forces in TCS can also be transformed to forces in FCN coordinate system using the transformation matrix T. (Refer section 2.4.3)

2.6.3 Post-Processor Module

In this module the data obtained from model namely—Ball-end mill geometry and tool orientation, variation of forces (in TCS and FCN) and torque are displayed in the GUI window. Following plots appear/displays on the GUI:

- Graphical representation of cutting edges on cutting tool envelope.
- Tool orientation in FCN coordinate system.
- Cutting forces as a function of angular rotation (θ) of the tool in TCS.
- Cutting forces as a function of angular rotation (θ) of the tool in FCN.
- Torque as a function of angular rotation (θ) of the tool in TCS.
- Maximum force variation for given Lead and tilt range.

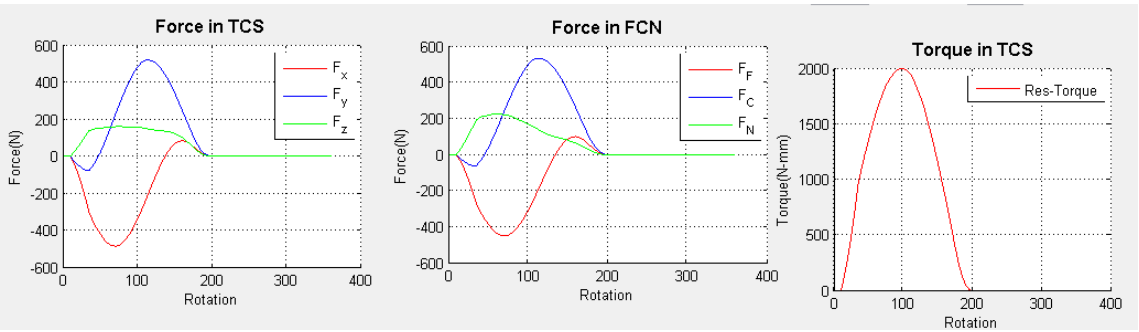

Figure 25 forces and torque outputs from MPS

2.6.4 Lead-Tilt Range Explorer:

The lead-tilt range explorer allows the user to identify optimal lead–tilt combinations which will minimize the cutting forces. The user needs to specify minimum and maximum values for lead and tilt angles. Based on these values, the ranges for lead and tilt angles are calculated and subsequently discretized to obtain a grid consisting of several combinations for lead and tilt angles. For each lead-tilt angle combination and given geometric and process parameters, the maximum value of F_x and F_y is found, and the resultant of both these forces is plotted. This process is repeated for all lead-tilt combinations and a three-dimensional data surface is plotted with Lead angle along the X-axis, tilt angle along the Y-axis, and the resultant of F_x and F_y plotted along the Z-axis.

By observing the profile of the data surface, the user can identify lead-tilt angle combination(s) where the resultant forces are minimum, and thus the actual milling process can be planned by selecting the parameters accordingly.

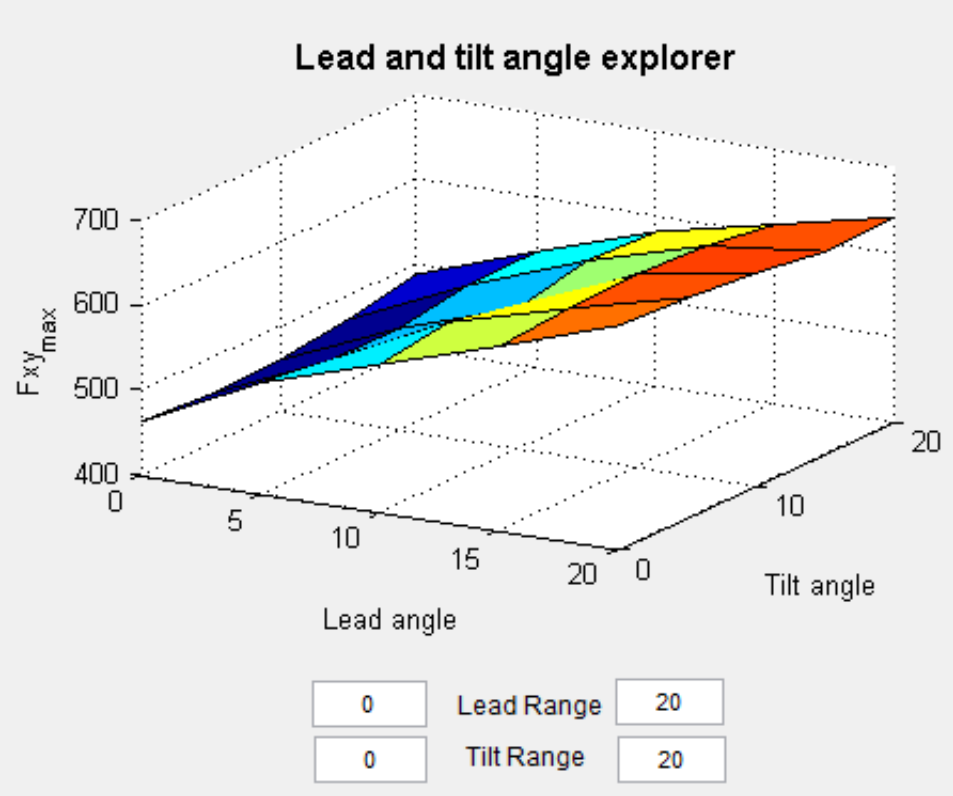

Figure 26 Lead and tilt angle explorer.

2.6.5 Limitations of MPS

Although the MPS program application is in its initial development phase, there are some current limitations:

- The cutting edges are only modelled for the ball end part of the tool. It is assumed that the shank part of the tool is not feeding the workpiece.
- The depth of cut (Input) given by the user should not be greater than the tool radius.
- The program is currently developed only for Titanium as the work material. The force and torque predictions may not be valid for other materials.
- The geometrical modeling assumes the workpiece to be flat and that the tool is performing a straight slot milling operation. Thus predictions will not be accurate for milling of free-form and/or partially machined surfaces.

###

3. METHODOLOGY B—ANALYTICAL MODEL BASED APPROACH

This is the second modeling methodology and it employs a physics based approach to model the metal cutting process. This model uses the *Unequal Shear-zone* theory to analyze the cutting mechanics of the chip shear-zone. It assumes the shear-zone to possess a fixed thickness as opposed to the single shear-plane model.

The *Johnson Cook Model* of shear failure in Oblique Cutting is implemented in order to calculate shear stresses and subsequently the forces on infinitesimal cutting elements of a ball end mill. On summation, these differential forces can give the net forces, torques acting on the cutting tool.

3.1 Unequal Shear-zone Theory

Merchant developed the simplest and widely used single-shear plane model based on the orthogonal cutting mechanics and minimum energy principle. It assumes that the deformation occurs on a single-shear plane, and this produces a velocity discontinuity along which the strain rate is infinite.

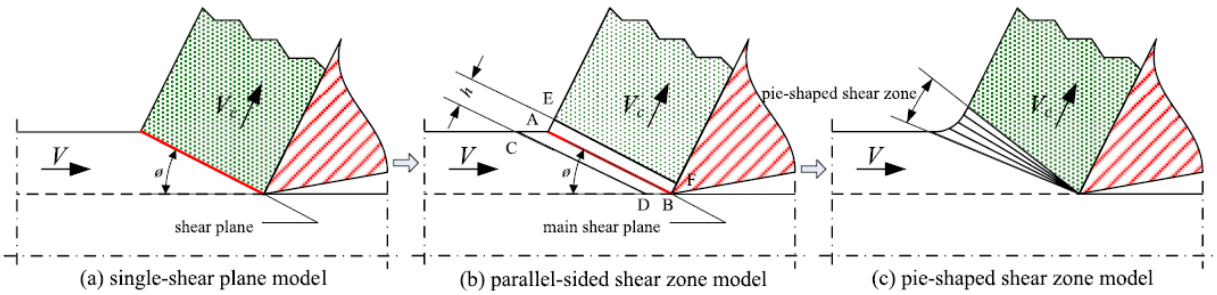

Figure 27 Different models describing the primary shear-zone

Though this model is simple and widely used, it has few drawbacks:

- The single-shear plane model does not consider the effect of strain, strain rate, and temperature on the material property. As a result it does not predict accurate results when applied to different work piece materials.

- Although geometric arguments can be used to compute an average effective strain rate, this assumption makes it difficult to include the effect of strain rate hardening, which is an important factor in high-speed machining processes.

To overcome these drawbacks a parallel-sided shear-zone model was introduced by Oxley and Welsh on the basis of chip formation observations. The new model possessed several aspects of the single-shear plane model, but also included effects of strain-hardening, strain-rate, and temperature on the material property. The Johnson-Cook model could now be used with parallel-sided shear-zone model to predict the flow stress distribution across the shear-zone, and subsequently the cutting forces.

Unequal Shear Zones

The parallel-sided shear zone model is based on the assumption that the shear-zone possesses a fixed thickness h (generally $h = 0.025mm$). As a result, there now exists a distribution of several mechanical characteristics such as the shear-strain, shear-strain rate, temperature, and flow stress across the thickness h.

The shear-plane along which the strain-rate is maximum is referred to as the *Main Shear plane*. However, the main shear plane is not located at the center of the shear-zone. It actually divides the shear-zone into two unequal parts characterized by the portion k. Thus it is located at a distance of kh from the base of the shear-zone, and is also the plane where the shear stress is maximum.

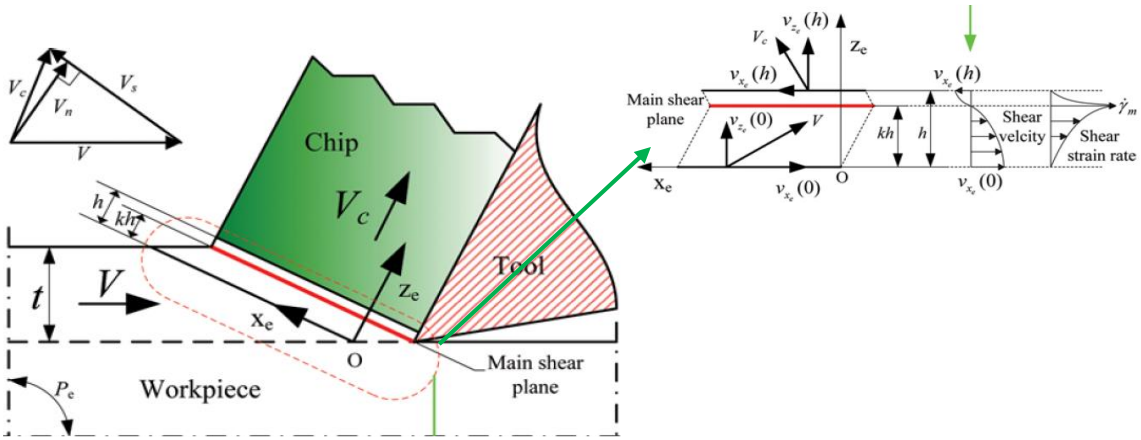

Figure 28 Unequal parallel sided shear-zone model

The parallel sided unequal division shear zone model is used in the subsequent analysis of oblique cutting mechanics. As shown in the above figure, V_{t0} and V_{th} are the tangential velocity components of the chip directed along the shear plane.

V_{n0} and V_{nh} are the normal velocity components of the chip directed along the normal to the shear plane. For simplicity it is assumed that all variables (velocity, temperature and stress) are functions of $\boldsymbol{z_e}$ only.

3.2 Oblique Cutting Process Model

In oblique cutting, as the cutting edge is inclined by a certain inclination angle to the direction of cutting velocity, several coordinate systems must be defined in-order to model all required directions of the cutting process.

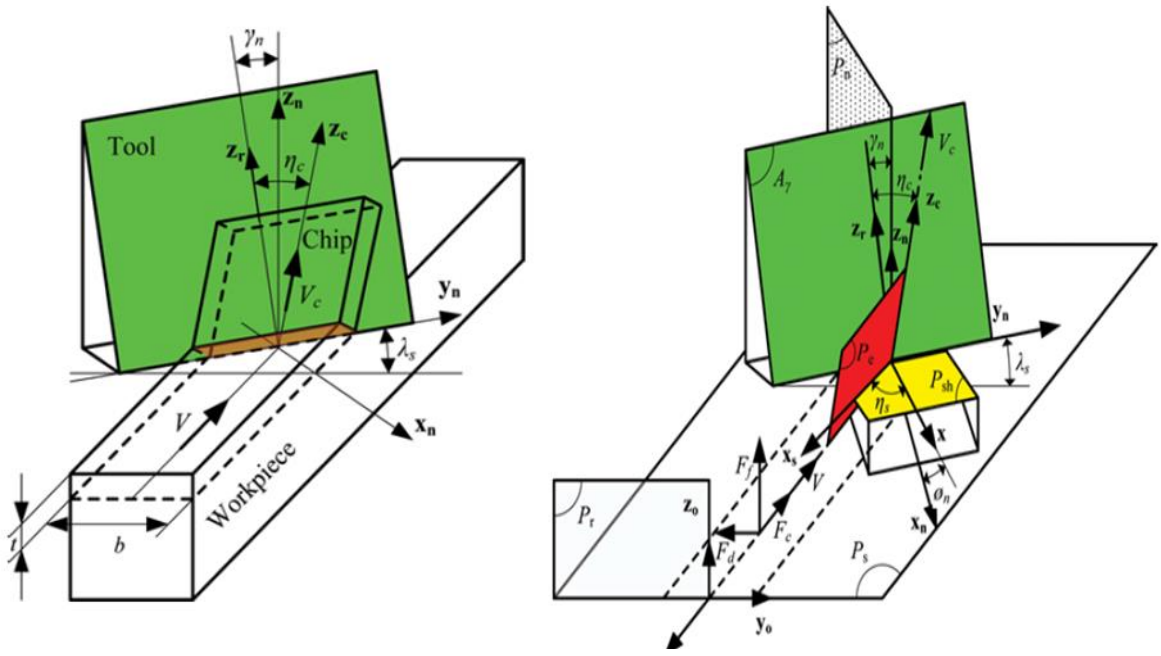

Figure 29 Oblique cutting and geometric coordinates systems

These coordinate systems are summarized in the following table:

Table 11 Coordinate systems and their characteristics

Coordinate Frame	Characteristics
$(\boldsymbol{x_o}, \boldsymbol{y_o}, \boldsymbol{z_o})$	• x_o is parallel to the cutting velocity direction • (y_o, z_o) is the reference plane $\boldsymbol{P_r}$, (x_o, y_o) is the cutting plane $\boldsymbol{P_s}$
$(\boldsymbol{x_n}, \boldsymbol{y_n}, \boldsymbol{z_n})$	• y_n is the cutting edge direction • (x_n, z_n) is the cutting plane $\boldsymbol{P_s}$ and z_n is parallel to z_0.
$(\boldsymbol{x_r}, \boldsymbol{y_r}, \boldsymbol{z_r})$	• $\boldsymbol{y_r}$ is collinear to $\boldsymbol{y_n}$ • $(\boldsymbol{y_r}, \boldsymbol{z_r})$ is the rake face $\boldsymbol{A_c}$ and $\boldsymbol{z_r}$ is perpendicular to $\boldsymbol{y_r}$.
$(\boldsymbol{x}, \boldsymbol{y}, \boldsymbol{z})$	• $\boldsymbol{y}$ is collinear to $\boldsymbol{y_n}$ • $(\boldsymbol{x}, \boldsymbol{z})$ is the normal plane $\boldsymbol{P_n}$, $\boldsymbol{z}$ is perpendicular to the shear plane $\boldsymbol{P_{sh}}$.
$(\boldsymbol{x_c}, \boldsymbol{y_c}, \boldsymbol{z_c})$	• $\boldsymbol{z_c}$ is the chip flow direction • $(\boldsymbol{y_c}, \boldsymbol{z_c})$ is the rake face $\boldsymbol{A_c}$ and $\boldsymbol{x_c}$ is collinear to $\boldsymbol{x_r}$.
$(\boldsymbol{x_s}, \boldsymbol{y_s}, \boldsymbol{z_s})$	• $\boldsymbol{x_s}$ is the shear flow direction • $(\boldsymbol{x_s}, \boldsymbol{y_s})$ is the shear plane $\boldsymbol{P_{sh}}$and $\boldsymbol{z_s}$ is collinear to $\boldsymbol{z}$.
$(\boldsymbol{x_e}, \boldsymbol{y_e}, \boldsymbol{z_e})$	• $\boldsymbol{x_e}$ is collinear to $\boldsymbol{x_s}$ • $(\boldsymbol{x_e}, \boldsymbol{z_e})$ is the equivalent plane $\boldsymbol{P_e}$ and $\boldsymbol{y_e}$ is perpendicular to the equivalent plane $\boldsymbol{P_e}$

3.2.1 Chip and Process Related Angles

In order to model the cutting process, certain angles must be defined which govern the flow of chips on the rake surface. These angles relate the rake surface definition and its orientation (with respect to the workpiece) to the chip flow direction.

The friction angle β and the chip flow angle η_c are calculated by simultaneously solving the following equations:

$$f(\beta) = \frac{V \cos\lambda_s(\tan(\phi_n - \gamma_n)\cos\gamma_n + \sin\gamma_n)}{\left(\frac{\tan\beta}{f_0}\right)^{\frac{1}{p}}} - \cos\eta_c$$

$$f(\eta_c) = \tan\eta_c \sin\phi_n \cos(\phi_n - \gamma_n) + cos\eta_c tan\lambda_s tan\beta \sin(\phi_n - \gamma_n)\cos(\phi_n - \gamma_n) + sin\eta_c tan\beta cos\gamma_n - sin\eta_c tan\beta sin\phi_n \sin(\phi_n - \gamma_n) - tan\lambda_s \cos^2(\phi_n - \gamma_n)$$

Subsequently, shear flow angle η_s, equivalent plane angle η_e, and the normal shear angle ϕ_n are calculated:

$$\eta_s = \tan^{-1}\left(\frac{tan\lambda_s \cos(\phi_n - \gamma_n) - tan\eta_c sin\phi_n)}{cos\gamma_n}\right)$$

$$\eta_e = \tan^{-1}\left(\frac{tan\eta_c \cos\eta_s + \sin\eta_s \sin(\phi_n - \gamma_n)}{\cos(\phi_n - \gamma_n)}\right)$$

$$\phi_n = \frac{\pi}{4} - \frac{\beta - \gamma_n}{2}$$

3.3 Constitutive Material Model

The constitutive material model essentially defines the behavior of the material when subjected to strain and temperature. The Johnson-Cook model is widely used to model metal cutting processes. It relates the flow-stress τ to the strain, strain-rate and temperature. It is expressed mathematically as:

$$\tau = \frac{1}{\sqrt{3}}\left(A + B\left(\frac{\gamma}{\sqrt{3}}\right)^n\right)\left(1 + C\ln\left(\frac{\dot{\gamma}}{\dot{\gamma}_0}\right)\right)\left(1 - \left(\frac{(T - T_r)}{T_m - T_r}\right)^m\right)$$

Here γ is the shear plastic strain, $\dot{\gamma}$ is the shear strain rate, $\dot{\gamma}_0$ is reference shear strain rate, T_m is melting temperature of the workpiece material, T_r is the reference temperature, T is the instantaneous temperature of workpiece. A is the material yield strength (MPa), B is the hardening modulus (MPa), C is strain rate sensitivity coefficient (viscosity), n is hardening coefficient, and m is thermal softening coefficient.

The first term in the above equation is the elasto-plastic term which represents the strain hardening. The second term is viscosity term which implies that flow stress increases when material is loaded with high strain-rate. The third term is the thermal softening term which reflects the decrease in the stress as the temperature increases.

3.3.1 Governing Equations for Strain-rate Distribution

The strain-rate is modelled as a piecewise power law distribution through the thickness of the shear zone.

$$\dot{\gamma} = \begin{cases} \dfrac{\dot{\gamma_m}}{(kh)^q} {z_e}^q & z_e \in [0, kh] \\ \dfrac{\dot{\gamma_m}}{(1-k)^q h^q} (h - z_e)^q & z_e \in [kh, h] \end{cases}$$

In the above equation, q is the parameter which characterizes with non-uniform distribution of the tangential velocity in the deformation zone k is the unequal division ratio. Furthermore, for the steady-state flow condition of a continuous chip, the strain variation is given as:

$$\dot{\gamma} = \frac{V cos\lambda_s sin\phi_n}{cos\eta_e} \frac{d\gamma}{dz_e}$$

3.3.2 Governing Equations for Strain Distribution

The above two equations are combined and integrated with respect to z_e to give the shear strain distribution as follows:

$$\gamma = \begin{cases} \dfrac{\dot{\gamma_m} \cos\eta_e}{(q+1)V \cos\lambda_s \sin\phi_n (kh)^q} {z_e}^{(q+1)} & z_e \in [0, kh] \\ -\dfrac{\dot{\gamma_m} \cos\eta_e}{(q+1)V \cos\lambda_s \sin\phi_n (1-k)^q h^q} (h - z_e)^{(q+1)} + \dfrac{\cos\lambda_s \cos\eta_e}{\cos(\phi_n - \gamma_n) \cos\eta_s \sin\phi_n} & \ldots z_e \in [kh, h] \end{cases}$$

Where

$$\dot{\gamma_m} = \frac{(q+1)V \cos\lambda_s \cos\gamma_n}{h \cos\eta_s \cos(\phi_n - \gamma_n)}$$

$$k = \frac{\cos(\phi_n - \gamma_n) \cos\eta_s (\cos\phi_n \cos\eta_s + \tan\lambda_s \sin\eta_s)}{\cos\gamma_n}$$

3.3.3 Governing Equation for Temperature

The heat transfer process during machining is governed by a two-dimensional heat flow equation. It is assumed the boundary of the shear band is adiabatic, the thermal conductivity is negligible, and the volumetric heat generated by conduction is zero. It is also assumed that the heat generation rate is due to plastic-deformation only. The heat transfer equation is expressed as:

$$\frac{dT}{dz_e} = \frac{\cos\eta_e}{\rho c V \sin\phi_n \cos\lambda_s} \mu\, \tau\dot{\gamma}$$

Here ρ is the work material density, c is the specific heat capacity, and μ is the Taylor-Quinney coefficient which represents the fraction of plastic work converted into heat. τ is the flow stress and $\dot{\gamma}$ is the shear-strain rate as described above.

The above equation is a first-order ordinary differential equation in T and z_e which is solved using numerical integration to give the temperature distribution in the shear zone.

The temperature distribution, along with the strain and strain-rate distributions, are used in the initial Johnson-Cook model to obtain the shear stress distribution τ across the primary shear zone. Furthermore, the shear stress τ_s acting on the main shear plane is also calculated.

3.4 Computation of Cutting Forces

In case of oblique cutting, there are forces acting along three mutually perpendicular directions, namely— Cutting force F_c acting along the cutting velocity $(\boldsymbol{x_o})$, feed force F_f along the workpiece normal $(\boldsymbol{z_o})$, and drift force F_d along $(\boldsymbol{y_o})$ due to the cutting edge inclination.

However, the above three forces are essentially resolved components of the forces acting in the shear zone. These are F_s and F_{ns} which represent the shear force and normal force on the main shear plane respectively. They are expressed mathematically as follows:

$$F_s = \frac{\tau_s}{\cos\lambda_s \sin\phi_n} tb$$

Where t is the uncut chip thickness, and b is the chip width, and τ_s is the shear stress acting on the main shear plane.

$$F_{ns} = \frac{cos\eta_s(\sin(\phi_n - \gamma_n) + cos\eta_c tan\beta \cos(\phi_n - \gamma_n))}{\cos(\phi_n - \gamma_n) - tan\beta \sin(\phi_n - \gamma_n)\, cos\eta_c} F_s$$

The three cutting force components(F_c, F_d, F_f) are then obtained as follows:

$$\begin{pmatrix} F_c \\ F_d \\ F_f \end{pmatrix} = \begin{pmatrix} \cos\eta_s \cos\phi_n \cos\lambda_s + \sin\eta_s \sin\lambda_s & \sin\phi_n \cos\lambda_s \\ \cos\eta_s \cos\phi_n \sin\lambda_s - \sin\eta_s \sin\lambda_s & \sin\phi_n \sin\lambda_s \\ -\cos\eta_s \sin\phi_n & \cos\phi_n \end{pmatrix} \begin{pmatrix} F_s \\ F_{ns} \end{pmatrix}$$

Where ϕ_n is the normal shear angle, λ_s is the cutting edge inclination angle, and η_s is the shear flow angle as described above.

To summarize, the following steps can be followed to compute the oblique cutting forces:

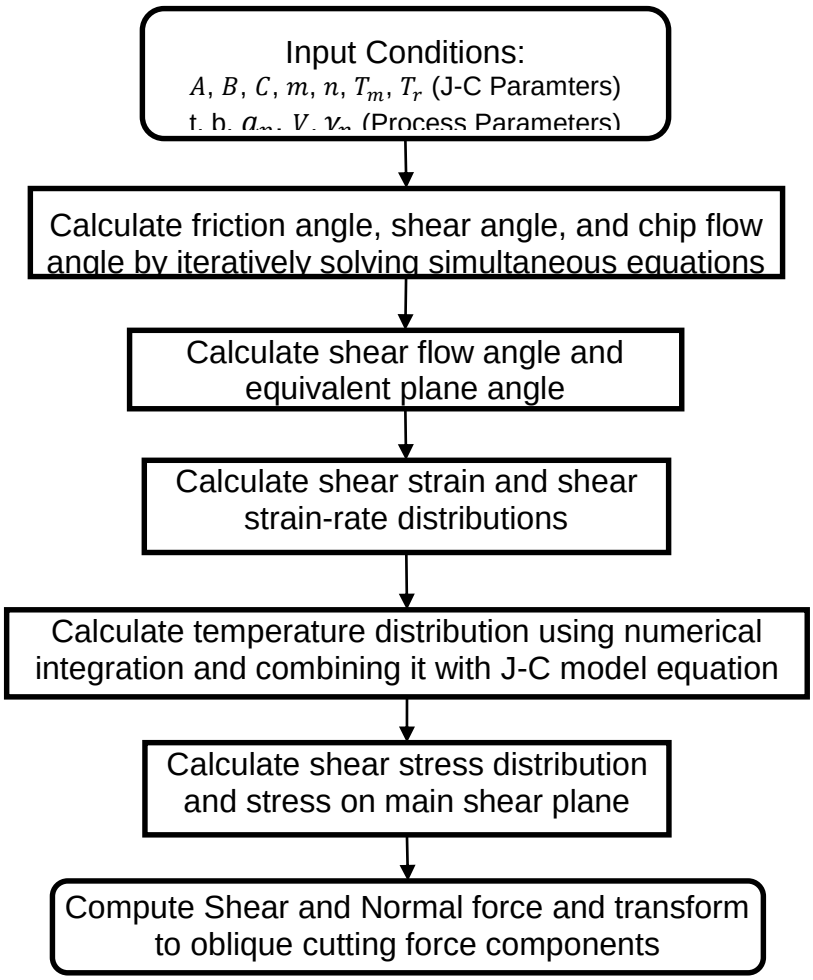

Figure 30 Flow Chart for Oblique Cutting Theory

3.5 Application to End-milling

The force model described in the previous is used to predict the cutting force acting on the tool performing end-milling. The geometry modeling of the tool is the same as described in the previous chapter. The helix angle i_o, and the tool diameter D is used to model the cutting edges of the tool. The cutting tool surface is then discretized into several points (which form cutting elements). Then based on the cutting depth and the feed direction, the discretized points undergoing cutting (i.e lying within the cutting zone) are identified and separated.

The identified points along with the milling feed rate is used to compute the differential length dS, width db and thickness $t_n$of the uncut chip. The differential chip dimensions, the cutting edge rake, and the inclination angle (derived from the helix angle) are used to compute the differential cutting forces dF_c, dF_d, dF_f as shown in the above flow-chart. Then the differential cutting forces in $\boldsymbol{x}, \boldsymbol{y}$, and $\boldsymbol{z}$ directions of the TCS are obtained by the following transformation:

$$\begin{Bmatrix} dF_x \\ dF_y \\ dF_z \end{Bmatrix}_{TCS} = \begin{bmatrix} -\sin(K)\sin(\Phi) & -\cos(\Phi) & -\cos(K)\sin(\Phi) \\ -\sin(K)\cos(\Phi) & \sin(\Phi) & -\cos(K)\cos(\Phi) \\ -\cos(K) & 0 & -\sin(K) \end{bmatrix} \begin{Bmatrix} dF_c \\ dF_d \\ dF_f \end{Bmatrix}$$

Here K is axial immersion angle and Φ radial immersion angle.

The above differential forces in TCS for all the cutting elements are then integrated to obtain the total cutting forces on the milling tools:

$$\begin{pmatrix} F_x \\ F_y \\ F_z \end{pmatrix} = \sum_{j=1}^{N} \sum_{s=1}^{K} \begin{pmatrix} dF_x \\ dF_y \\ dF_z \end{pmatrix}_{j,s}$$

N, and K are the number of angular and axial increments in which the cutting tool is discretized.

3.6 Experimental Validation

The model described above was used to predict cutting forces during flat-end milling of Inconel-718. The geometry module was modified in-order to model the cutting-elements for a flat-end mill. The predicted force data were then validated against experimental data. The tool geometry and process parameters are as follows:

- Tool type: Helical flat-end mill
- Tool diameter: 8 mm
- Number of cutting flutes: 2
- Radial rake angle: 17°
- Helix angle: 30°

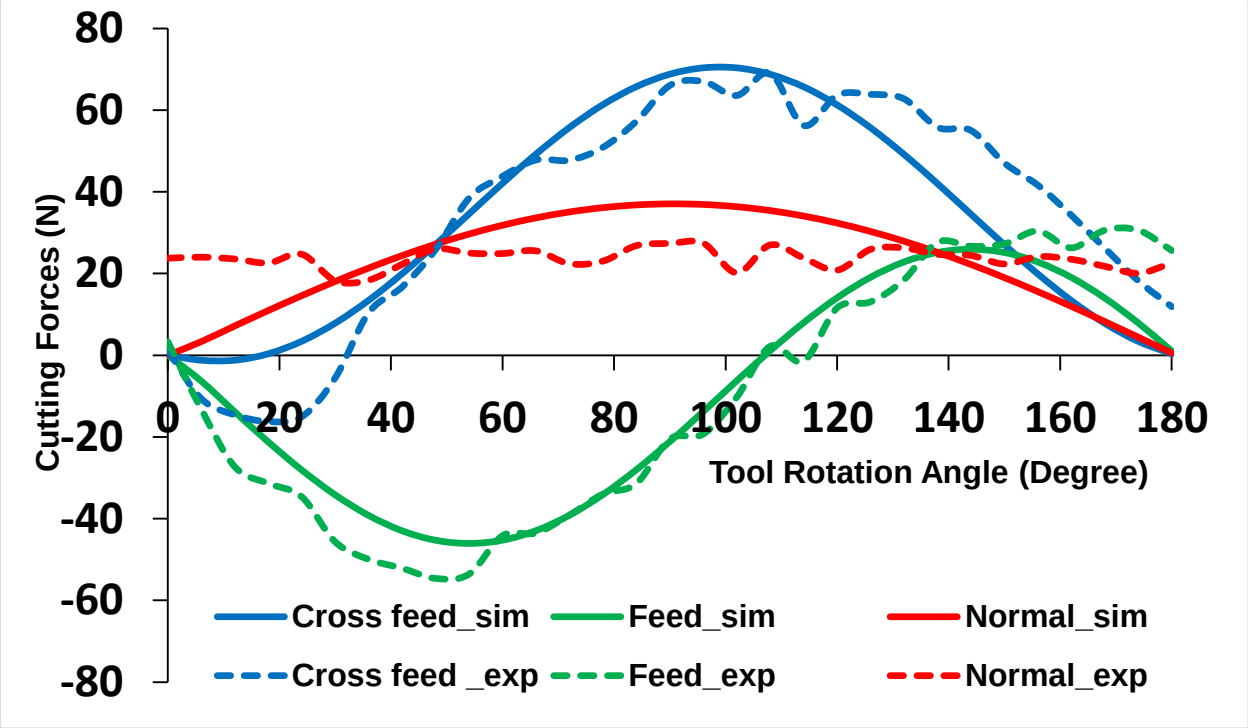

Figure 31 Experimental Validation Study

Although the experimental data is 'noisy', it can be observed that the force model satisfactorily predicts the cutting forces. However, this model needs further validation and additional experimental tests will be performed.

###

4. CONCLUSIONS AND FUTURE WORK

As outlined in the beginning, the objective of this project is to analytically model the forces generated during multi-axis machining operations. To this end, two methodologies have been developed which are used to model the forces and toque acting on the cutting tool during multi-axis milling processes.

One of the methodologies is based on an empirical mechanistic approach in which the basic orthogonal cutting parameters of the shear-zone are estimated using regression curve-fitting on several measured cutting test results. The other methodology employs a physics-based analytical modeling approach in which the deformation behavior of the material undergoing cutting is predicted using the Johnson-Cook material model.

Both of these methodologies follow a modular approach to model the forces. The tool geometry, its orientation, and the workpiece geometry are modelled parametrically using various mathematical formulations. Subsequently, based on the input machining parameters, the cutting-zone is identified.

The two methodologies mentioned above are used to develop the constitutive material model which is then used with user-specified machining process parameters, and the identified cutting-zone are used as inputs to the Traction model. The traction model is then run to predict the cutting forces and torque as function of the tool rotation.

From the validation studies performed on both methodologies, it can be concluded that the traction models predict the forces with fairly good accuracy. However, there are few limitations that need to be addressed.

- The current models are developed only for cylindrical ball-end milling tools. These have to be extended in-order to model a variety of other tools such as—conical ball-nose end-mill, bull-nose end mills and others.
- It is assumed the workpiece is flat and the tool is performing a straight slot milling operation. Thus the geometric modeling of the cutting-zone has to be extended to incorporate workpieces having free-form surfaces with pre-cut slots from previous tool passes.

- The models have been currently developed and validated only for Titanium and Inconel. However they must be extended to include other materials such as Aluminum, Steel and others.
- The effect of temperature is not extensively incorporated in these models. Thus thermos-mechanical effects must be built into the models.

Apart from the limitations listed above, there is immense scope to extend the models much further. Some of these aspects are as follows:

- The forces obtained from the model can be used to study vibrations and chatter that are associated with high speed machining processes. This analysis can be used to optimize machining parameters and design tools so as to reduce or dampen vibrations. As the vibrations are minimized, the surface quality of the machined parts can be further improved.
- Tool wear analysis can be performed using the cutting forces obtained from the model. Based on the analysis, designated cutting tools can be designed so as to minimize tool wear for specific milling operations and toolpaths. This will not only help to improve tool-life but also improve the surface quality.
- The force model can be integrated with toolpath planning algorithms. Conventionally, toolpath algorithms are developed in order to remove excess material from the stock to reach the desired part shape in the least possible time. However, they do not take into account material characteristics, and as a results toolpaths may be generated which lead to higher cutting forces and faster tool wear-out. By integrating toolpath algorithms with the force model, the generated toolpaths will not only be optimized for least machining time but also for reduced cutting force, torque, and tool-wear. Doing so will help to improve the overall productivity of machining, thereby reducing process time, as well as improving the quality of finished parts.

###

REFERENCES

1. Lee, P. and Altintas, Y., PREDICTION OF BALL END MILLING FORCES FROM ORTHOGONAL CUTTING DATA, International journal of machine tools and manufacture 36 (1996) No.9 1059-1072.
2. Ozturk, E. and Budak, E.,: MODELLING OF 5 AXIS MILLING PROCESSES, MACHINING SCIENCE AND TECHNOLOGY (2007) 11(3) 287-311.
   Machining science and technology: An international journal
3. Ozturk, E.,Tunc,T.,Budak, E.,: INVESTIGATION OF LEAD AND TILT ANGLES EFFECT IN 5-AXIS BALL-END MILLING PROCESSES, International journal of machine tools and manufacture,49 (2009) 1053-1062
4. Altintas Y.,: *Manufacturing Automation: Metal Cutting Mechanics, Machine Tool Vibrations, and CNC Design*, Cambridge University Press, Second edition 2012**.**
5. Li, B. Wang, X. et al, 'ANALYTICAL PREDICTION OF CUTTING FORCES IN ORTHOGONAL CUTTING USING UNEQUAL DIVISION SHEAR-ZONE MODEL, International Journal of Advanced Manufacturing Technology, 54 (2011) 431-443
6. Binglin Li , Yujin Hu , Xuelin Wang , Chenggang Li & Xingxing Li AN ANALYTICAL MODEL OF OBLIQUE CUTTING WITH APPLICATION TO END MILLING, Machining Science and Technology: An International Journal, 15:4 (2011), 453-484

###